A CONSTITUTIVE EQUATION FOR COLLAGEN FIBERS

Thesis for the Degree of Ph. D.
MICHIGAN STATE UNIVERSITY
ROGER C. HAUT
1971

This is to certify that the

thesis entitled

A CONSTITUTIVE EQUATION FOR COLLAGEN FIBERS

presented by

Roger C. Haut

has been accepted towards fulfillment
of the requirements for

Ph.D. degree in Mechanics

Robert Lee Sattler

Major professor

Date July 21, 1971

O-7639

ABSTRACT

A CONSTITUTIVE EQUATION FOR COLLAGEN FIBERS

By

Roger C. Haut

The purpose of this research is to develop a constitutive equation for collagen fibers, and to compare the results of a number of basic tests with the mathematical model. The collagen was obtained in a pure form by the extraction of fiber bundles from the tails of mature rats, and the specimens were immersed during testing in a constant temperature saline bath. Three types of basic tests were conducted on the fiber bundles. The first test series were relaxation tests at various levels of strain. A second series of loading and unloading cycles were performed at different strain rates. A third series of tests were conducted for a sinusoidal strain of various amplitudes and frequencies.

A "quasi-linear" viscoelasticity law has been developed based on a suggestion presented by Y. C. Fung. From the results of the relaxation tests the material

constants in this equation were determined and the constitutive equation was then used to predict the results of constant strain rate tests, hysteresis loops, and sinusoidal tests.

A CONSTITUTIVE EQUATION FOR COLLAGEN FIBERS

By

Roger C. Haut

A THESIS

Submitted to
Michigan State University
in partial fulfillment of the requirements
for the degree of

DOCTOR OF PHILOSOPHY

Department of Metallurgy, Mechanics, and Material Science

1971

ACKNOWLEDGMENTS

The author wishes to express his appreciation to the following people for making this phase of his graduate work possible:

To Dr. Robert W. Little, his major advisor, for his encouragement, friendship, and, most of all, for his valuable assistance in the preparation of this thesis.

To the National Science Foundation for its financial support during his graduate work.

To the Division of Engineering Research for the finances required for the experimental equipment.

To his mother for her encouragement throughout his academic years.

To his wife's parents for their understanding during his graduate work.

To his wife, Judy, for her endless patience and encouragement throughout his graduate work.

TABLE OF CONTENTS

	Page
LIST OF TABLES	iv
LIST OF FIGURES	v
I. INTRODUCTION	1
1. Biological Tissues--General	1
2. Formation and Structure of Collagen	3
3. Mechanical Properties of Collagen	10
II. SURVEY OF LITERATURE	12
III. EXPERIMENTAL METHODS	19
IV. MATHEMATICAL FORMULATION	28
1. Relaxation Test	30
2. Constant Strain Rate Test	31
3. Sinusoidal Test	33
V. PRESENTATION OF RESULTS	37
VI. CONCLUSIONS	59
BIBLIOGRAPHY	62

LIST OF TABLES

Table		Page
1.	Experimental Results of Relaxation Tests at Different Strain Levels	41
2.	Experimental Constants from Constant Strain Rate Tests ($\sigma = B\varepsilon^A$)	42
3.	Experimental Constants from Sinusoidal Tests	43

LIST OF FIGURES

Figure		Page
1.1	The Molecular Chain of Collagen	5
1.2	The Collagen Fibril	6
3.1	Experimental Stress Relaxation Test	23
3.2	Cyclic Test	24
3.4	Collagen Fiber Bundles	25
3.5	Fiber Immersed in Saline Bath	25
3.6	Experimental Setup	26
3.7	Specimen Grips	26
3.8	Tensile Testing Fixture	27
3.9	Sinusoidal Test Fixture	27
5.1	Stress-Strain Plot at Various Strain Rates .	44
5.2	Stress-Strain Plot for 3.6%/min. Strain Rate	45
5.3	Stress-Strain Plot for 9.2%/min. Strain Rate	46
5.4	Stress-Strain Plot for 18.7%/min. Strain Rate	47
5.5	Stress-Strain Plot for 22.6%/min. Strain Rate	48
5.6	Stress-Strain Plot for 30.9%/min. Strain Rate	49
5.7	Stress-Strain Plot for 45.0%/min. Strain Rate	50
5.8	Hysteresis Loop at 3.6%/min. Strain Rate . .	51
5.9	Hysteresis Loop at 22.6%/min. Strain Rate .	52

Figure		Page
5.10	Hysteresis Loop at 45.0%/min. Strain Rate . .	53
5.11	Load Decay During Sinusoidal Extension . . .	54
5.12	Plot of Stress Amplitude vs. Cycle Number at a Frequency of 3.3 rad./min. and a Strain Amplitude of 1.8%	55
5.13	Plot of Stress Amplitude vs. Cycle Number at a Frequency of 77.0 rad./min. and a Strain Amplitude of 1.8%	56
5.14	Plot of Stress Amplitude vs. Cycle Number at a Frequency of 31.6 rad./min. and a Strain Amplitude of 1.2%	57
5.15	Plot of Stress Amplitude vs. Cycle Number at a Frequency of 31.6 rad./min. and a Strain Amplitude of 0.6%	58

I. INTRODUCTION

1. Biological Tissues--General

All living organisms are composed of small units called cells. When similar cells are joined together, either closely or loosely, with an intervening non-cellular material, the aggregate is called a tissue. In the animal kingdom there exist four primary types of tissues: epithelial, connective, muscle, and nervous tissue. Epithelial tissue is the predominant type of tissue in most free internal and external surfaces. The cells of this type of tissue are closely joined, hence there is a minimum quantity of intercellular material. Epithelial tissue is further subdivided by its cellular shape. The epithelial surface which lines the mouth, esophagus, the outer surface of the cornea, and most of the female urogenital tract is called squamous epithelium because of its thin flat plate-like cells. Columnar, which are rectangular as the name suggests, constitute areas such as the pharynx, soft palate, and gland ducts. Cuboidal epithelium tissue is found in the kidneys, the retina of the eye, and on the inner surface of the lens of the eye.

Muscle tissue, known for its contractibility and irritability, has a cellular structure in which the cells are elongated into muscle fibers. The contractibility of this particular type of tissue is theorized as being attributed to a dove-tailing effect of its fibers, myosin and actin.

Nervous tissue is composed of nerve cells, or neurons, and some supporting cellular structures. Nerve impulses, according to the Membrane Theory, are conducted by a depolarization of charge along the tubular membrane of the neuron. These impulses are then transferred from one neuron to the next neuron via a synapse. At a synapse there is no physical contact of the neurons, therefore this contact has been theorized to be of an electrical or chemical nature.

Connective tissue is by far the most predominate and diversified tissue in the entire animal kingdom. With reference to the human body, connective tissue appears as bone, cartilage, ligaments, mesentery, and tendons. Blood is also classified as a type of connective tissue. The distinguishing characteristic of this type of tissue is the presence of a large amount of intercellular material. This intercellular material may consist of collagenous or white fibers, elastic or yellow fibers, reticular fibers, and varying amounts of an amorphous ground substance. Elastic fibers are rather long, flat ribbons which contain

a substance called elastin. The low modulus fiber elastin is the material which gives certain ligaments, namely the ligamentum nuchae, the ability for large deformations as seen in the neck region of grazing animals. Although elastic fibers exist in most connective tissues, the collagenous fibers tend to have the major effect on the mechanical properties of these tissues. Reticular fibers are thought to be immature collagen fibers.

The importance of collagen is displayed in the fact that connective tissues are classified according to the amount and orientation of its collagenous fibers. Loose connective tissue contains reticular, elastic, and collagenous fibers. The matrix of intercellular material has no orientation of its fibers, resulting in a low modulus material such as the mesentery of the abdomen. Dense connective tissue is essentially the same as loose connective tissue except for a fewer number of cells and a larger percentage of collagen fibers. Cartilage and bone are classified as this type of connective tissue. Regular connective tissue has an abundance of collagenous fibers, and has a definite arrangement of its fibers.

2. Formation and Structure of Collagen

Collagen is the major constituent of most connective tissues, and much research has been directed toward a better understanding of its function in tissues.

Collagen is perhaps the most abundant protein in the body. It is a simple protein in that upon cleavage only amino acids are formed. The basic collagen molecule is a group of three polypeptide chains each composed of thousands of amino acid units linked together. In ordinary simple proteins the chains are assembled from the standard assortment of the known twenty-two amino acids which exist in the body, and once linked together end to end the acids are not further altered. In the synthesis of collagen, however, two unusual amino acids, hydroxyproline and hydroxylysine, seem to be formed after the molecular chain has been assembled. These new amino acids are created by the addition of hydroxyl groups to some of the proline and lysine units in the chain. This is a characteristic of the collagen protein which has not been observed in the synthesis of other proteins (1). In collagen about twenty-five percent of the links are proline and hydroxyproline giving the molecule a high resistance to heat and chemical denaturation. Glycine appears to occupy about thirty percent of the collagen molecule. A further characteristic of the collagen molecule is the physical orientation of the molecular chains. The basic molecular chain is twisted into a left-handed helix and three such helices are wrapped around each other to form a right-handed superhelix. These chains are held together by hydrogen bonds.

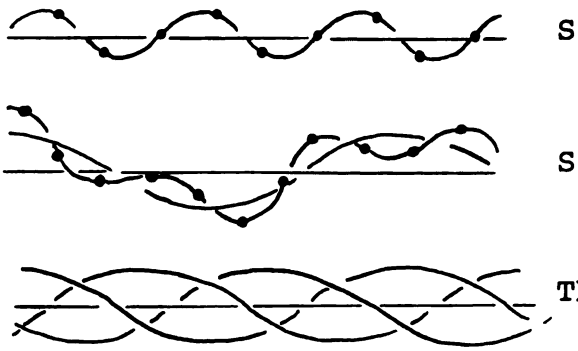

Fig. 1.1 The Molecular Chain of Collagen

Early investigation into the structure of the collagen molecule displayed a characteristic periodicity of approximately seven hundred angstroms. This value was determined by the bands seen in electron micrographs of collagen fibrils. These bands were assumed to be the lengths of the primary collagen molecules (2). In the tests performed by Schmitt, in which he developed techniques for experimentally reconstituting collagen from solutions, this periodicity of seven hundred angstroms was again observed. Several years later workers in Russia found certain needle-like entities when they observed reconstituted collagen under a light microscope. These new entities have a periodicity of 2800 angstroms. Therefore they called this new structure "fibrous long spacing." Later it was found that collagen could be recrystallized into still a third type of structure called "segmented long spacing," which also had a periodicity of 2800

angstroms but this form was not fibrous. With further reconstitution experiments it was determined that all three structures could be dissolved, and converted into either of the other forms. It was then concluded that all forms were being constructed from threadlike units about 2800 angstroms long and less than 15 angstroms wide. These units were later given the name tropocollagen. In the native collagen fibril the 700 angstrom periodicity is obtained by these tropocollagen macromolecules lining up in the same direction and overlapping by about one-quarter of their length. The collagen fibril then has a characteristic periodicity of 700 angstroms and approximately 500 angstroms in diameter.

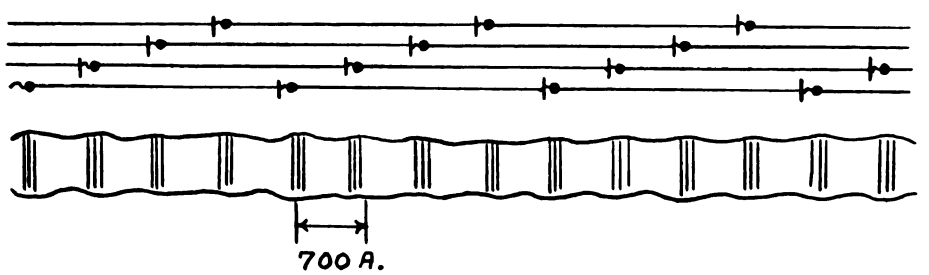

Fig. 1.2 The Collagen Fibril

As a result of the studies made on the formation of these three forms of collagen, it is now possible to give a reasonable explanation of the formation of collagen by the cells known as fibroblasts. Insight into the

problem was gained by observing that a certain fraction of the collagen from young animals could be dissolved by a cold neutral salt solution, and simply by warming the solution to body temperature fibrils with a native periodicity could be obtained (3). These and other studies on the aging of collagen suggested that the fibroblast evidently synthesizes the complete tropocollagen molecules and extrudes them into the extracellular space, where they form fibrils. Although this formation may require heat and time, other substances in the extracellular environment may play a regulatory role.

These collagen fibrils are regarded as the basic unit found in all forms of connective tissue (4,5). The division of collagenous tissues into various dimensional levels, by utilizing light and electron microscopy, has caused much confusion. Even the term fibril, given previously to a unit which has a diameter of approximately 500 angstroms is called a microfibril by some (6). Much of this confusion is a direct result of the variation in size of this unit between different species and tissues. For example, the diameter of these fibrils varies between 300 and 1300 angstroms in man and from 1600 to 4000 angstroms in the kangaroo (5). Ham, in his discussion of loose connective tissue, gives a value of approximately 400 angstroms for the microfibrils. In histological references the term fiber appears, however, there does not seem to be a precise

definition for these threadlike units. When reference is made to collagen, Ham uses the definition of "fiber" as that structure which has a diameter between 1 and 12 microns (6). He proposes that collagen fibers are composed of parallel fibrils, which have diameters ranging from 0.3 to 0.5 microns, lying side by side to form the fiber.

Tendonous tissues are tissues which have a large number of bundles of collagen running a somewhat parallel course (5,7). Whether these bundles are composed of the fibril or fiber units is questionable. Similar bundles have diameters of 1 to 2 microns in loose connective tissue; 10 to 40 microns in skin; and up to 300 microns in tendons (5). These bundles of collagen are called primary tendon bundles (5,8), collagen fiber bundles (7), collagen fibril bundles (3), or just tendon fibers (4,8,9). The bundles are described as having a helical or wavy appearance (8,9). By Ham's definition these units would be termed fibrils.

Two tissues which have received much investigation recently are the mesentery and fascia. Fascia is a tissue intermediate between loose and dense connective tissue. The collagen fiber bundles are smaller in size in these tissues than tendon bundles, and they are arranged regularly in multiple sheets following a parallel and often wavy course. Mesentery is a loose connective tissue

which is pictured as a randomly oriented two dimensional network. The collagen bundles in it vary in size, but are smaller than primary tendon bundles. In tendons the primary tendon bundles are grouped into secondary bundles with a diameter of approximately 600 microns. The arrangement within secondary bundles is a ropelike twisting of fibers around each other (8). The epitenon, a delicate layer of loose connective tissue covering a tendon, continues into its interior as the endotenon, intervening between the component bundles and carrying small blood vessels, lymphatics, and nerves. Since tendons originate from groups of fibroblasts, which as they mature form fibers and become dormant fibrocytes, there is also a number of these dormant cells existing in a tendon. The tendon is often termed as a non-living material due to its small blood supply.

Another extracellular material existing in connective tissues is an amorphous ground substance. This substance, comprising about one percent of a tendon, is a gel lying between the fibrillar elements and containing the acid mucopolysaccharide hyaluronic acid, some sulfated mucopolysaccharides, and other carbohydrates (5). The physiological function of this ground substance, as seen in loose connective tissue, is to serve as an intermediate material by which epithelial cells are nourished and waste products disposed (6).

A pure form of collagen bundles can be easily obtained from the tail tendons of cats, kangaroos, and rats. Unlike most other connective tissues which have other constituent fibers and ground substances, tail tendons are a source of almost pure collagen. The primary tendon bundles parallel the tail with no interweaving. The bundles are loosely connected and are therefore easily excised with little or no force. The tendons lie directly under the skin, and are surrounded by a loose connective tissue sheath which is attached to the vertebrae of the tail by elastic fibers (8). Originating on the trunk the tendons run the entire length of the tail with the component bundles having a rather uniform diameter throughout their length. Being approximately 95% pure collagen, tests conducted on this material will serve as a basis for studies on more complex tissues.

3. Mechanical Properties of Collagen

There are many problems in physiology whose solutions require a detailed knowledge of the mechanical properties of the tissues involved. The majority of these problems deal with connective tissues such as mesentery, blood vessels, skin, tendons, ligaments, and cornea. Since these tissues are composed of various amounts of fibrous and amorphous materials, connective tissues may be treated as fiber-reinforced composites. A complete

study of these tissues must, therefore, begin with an understanding of the mechanical properties of their constituent fibers and matrix materials. Because of the difficulty encountered in the dissection of these components from the tissues, much research deals with tissues in which one of the components is predominant. In ligaments such as ligamentum nuchae, the elastic fiber is the most predominant. Tendons are the best source of collagen. In particular, the tail tendons of rats offer a source of almost pure collagen fiber bundles. It is generally agreed in the literature that the major stress-bearing component of connective tissues is the collagen fiber bundle. Many of the problems of aging and disease of connective tissues have been traced to the collagen fibers. Because of the major role played by collagen in connective tissues, its mechanical properties are of interest.

II. SURVEY OF LITERATURE

The majority of the early research dealing with the mechanical properties of biological tissues involves studies of the tensile strengths of ligaments and tendons. One of the first such studies was made by A. E. Cronkite in 1935 (10). He indicated that for tendons preserved in a "normal physiological" manner there was no one tendon that was consistently stronger than another, but that there was a slight increase in tensile strength with diameter. Values for all tendons ranged from 2.8×10^8 dynes/cm.^{2} to 2.1×10^9 dynes/cm.^{2}. In a similar study E. H. Harris reported that for embalmed flexor digitorum tendons the average Young's Modulus was 7.6×10^9 dynes/cm.^{2} (11). C. M. Gratz reported values of 6.8×10^8 dynes/cm.^{2} for the tensile strength and 3.9×10^8 dynes/cm.^{2} for Young's Modulus of Achilles tendons immersed in Ringer's solution (12). Similarly, he reports a tensile strength of 7.3×10^8 dynes/cm.^{2} with modulus of 3.4×10^8 dynes/cm.^{2} for flexor digitorum tendons, and a strength of 6.7×10^8 dynes/cm.^{2} for the erector spinae tendon. L. B. Walker states values of from 7.3×10^8 dynes/cm.^{2} to 1.5×10^9 dynes/cm.^{2} for human plantaris tendons.

A number of investigations have dealt with the problem of testing environments. In 1954, J. W. Smith stated that he found drastic effects on the strength of anterior cruciate ligaments for times of more than 30 minutes after death of the animal (12). A. Vidik reported that parameters such as the slope of the load-elongation curve, failure energy, failure load, and elongation at failure varied from the fresh control group for specimens stored in saline, embalmed, or frozen (13). Variations in some mechanical properties with relative humidity and temperature have also been studied (9,14). Most authors agree that for temperatures below 40° C. there is no dependence of temperature on the mechanical properties. However, Rigby reported drastic effects on the mechanical properties of rat tail tendons for temperatures above 40° C.

Examinations of the shape of the stress-strain curves for biological materials began with a paper by Rigby (9). He performed various tests on rat tail tendons which were immersed in a saline bath. In agreement with recent authors Rigby found a nonlinear relationship existing between stress and strain. Using polarized light he noted that the loss of initial nonlinearity in the curves coincided with the straightening of fibers which were previously wavy. This waviness of the fibers initially was described as being of a helical nature by Verzar (8).

Rigby found that by carefully dissecting the rat tail tendon a helical structure could not exist, and attributed Verzar's error to improper illumination techniques. Since Rigby's work, many authors have studied collagenous tissues and found that the nonlinear stress-strain curves for these tissues are described with the straightening of this wavy pattern. Abrahams cites three distinct regions in the stress-strain curve for human tendons (26). He found by histological techniques that the first region to 1.5% strain involved the straightening of the wavy fibers. A second region of 1.5% to 3.0% shows oriented fibers, whereas in the third region the response is linear for fibers which are fully oriented. According to Elliot the normal physiological range of transmitted tensions appears to lie in the early nonlinear region (5). From his work on penniform and fusiform muscles he found that the waveform disappeared in the tendons at 200 grams/mm.^{2}, whereas the muscles were capable of tetanic tensions to 2.5 kg./mm.^{2}. Other workers suggest that tendons are never stressed in vivo to greater than one-quarter of their ultimate strength (15,16,17). Both Abrahams and Rigby state a value of less than 3% strain for normal physiological activity of tendons. In Rigby's tests a permanent set was noticed when these fibers were stretched to more than 2%. Likewise, Abrahams found that tendons began to fail if a safe limit of approximately 4% was exceeded.

F. R. Morgan performed a series of tests on raw and tanned leather collagen fibers at various levels of relative humidity (18). For a loading rate of 6 grams per minute in various humidities the experimental data could be fit with a power function. He stated a value of approximately 1.3 for the power of strain which fit the data. In another series of tests on rat tail tendons conducted by H. Elden, the power function was again found to fit the experimental data quite well (3). These results indicate that for strains less than two percent, the stress can be approximated by the square of the level of strain. P. L. Blatz has further indicated that a power function fits data for tests on frog's striated muscle, human papillary muscle, and cat's mesentery (19). Further test data for the skin of a rat was also given by Elden. He observed that for rat skin the initial linearity of the stress-strain plot abruptly became nonlinear at a certain critical strain level of approximately three percent. It has been verified by histological analysis that it is at this critical strain that the skin collagen fibers begin to extend. By extrapolating the early linear region beyond the critical strain, Elden found that the net stress increased linearly with the square of the strain above this level. The entire stress-strain curve was then proposed to be a composite of an early linear region and a secondary region in which the stress increased as the square of the strain.

In 1967, Y. C. Fung proposed an exponential equation for tests conducted on the mesentery of rabbits (20). The tests were conducted in a step manner with a relaxation period following each step increase in strain level. These tests indicated that the slope of the stress-extension curve was proportional to a linear function of the stress level after relaxation. After integration of this equation and incorporation of a zero factor, taken from the theory of finite elasticity, Fung proposed an equation of the form

$$\sigma = D[\lambda - \frac{1}{\lambda^2}]e^{b\lambda}$$

where D and b are constants, and λ is the extension ratio. This was termed the "elastic" constitutive equation. Recently, D. D. Stromberg has conducted tests on rat tail tendons in which he loaded the specimens with step increases in load (21). After allowing the specimens to creep at each level of load, he found that an "elastic" curve similar to that proposed by Y. C. Fung fit the data. He further examined the results of past experiments and gave values for the exponential constant in Fung's equation for other tissues. The values of this constant were 450 for primary tendon bundles, 120 for whole human tendon, 25 for human plantar fascia, and 12 for rabbit mesentery. This correlation indicated that the value of Fung's modulus might be proportional to the amount and degree of orientation of the collagen fibers.

In a study performed by the author on the anterior cruciate ligament of canines a similar exponential equation was predicted from tests conducted similar to Fung (22). However, this equation was also dependent on the rate of strain used for the steps. The equation was of the form

$$\sigma = f(\dot{\varepsilon})[\varepsilon-\varepsilon^2]e^{a\varepsilon}$$

where a is a constant. Although no further analysis of time effects was included, the results did indicate that this parameter must be included in the formulation of a constitutive equation for biological tissues. The major effect of increasing the rate of strain or stress on biological tissues is to shift the curves toward the stress axis with no apparent change in the shape of the curve (9,22,23,25,26). In the works of Rigby and Abrahams it was mentioned that for a relaxation test, the stress appeared to decay as a linear function of the logarithm of time. There has been a number of recent attempts at modeling the viscoelastic properties of biological tissues with discrete linear viscoelastic parameters (25,27,28). For the most part these attempts have failed because of the nonlinear nature of these properties and the inherent limitations of discrete model analysis. A possible alternative to the discrete model analysis has been suggested by Y. C. Fung (29). Fung proposed that it might be

possible to describe the stress-strain-history law of biological tissues in the form of a "quasi-linear" visco-elasticity law;

$$\sigma(t) = \int_0^t G(t-t') \frac{d\sigma^e[\lambda(t')]}{d\lambda} \frac{d\lambda(t')}{dt'} dt'$$

where σ is the stress, σ^e is the "elastic" response, λ is the extension ratio, and $G(t)$ is a "reduced" relaxation function. This equation is linear with respect to σ^e, but is nonlinear with respect to $\lambda(t)$ if σ^e is a nonlinear function of λ.

III. EXPERIMENTAL METHODS

In order to study the uniaxial stress-strain-history response of collagen fibers, the specimens were subjected to three different uniaxial tests. Relaxation tests were conducted at various levels of strain. By the loading and unloading of the specimens at a constant strain rate, hysteresis loops were obtained. The response of collagen fibers to a sinusoidal strain was considered in the third series of tests. The results of these tests were then used to establish a uniaxial constitutive equation for collagen.

Collagen fiber bundles were obtained from 350-375 gram male albino rats of the Sprague-Dawley strain. The animals were killed with ether, and the tails were immediately cut off at the base. Within 30 minutes after death the tails were cut at approximately three centimeters from the distal end, and the bundles carefully pulled from the tendon sheath. Only those bundles which pulled out with little or no force were used for this study. From the four bands of collagen bundles in the tail section approximately 20 specimens of rather uniform dimensions were extracted. These bundles had diameters of approximately 200 microns and lengths of about 10 centimeters

(Fig. 3.4). Immediately after extraction the specimens were immersed in Lock's saline solution at room temperature. The saline solution was prepared in 18-liter quantities according to the following formula:

1. 7.56 grams of KCL per 18 liters of water.
2. 2.70 grams of $NaHCO_3$ per 18 liters of water.
3. 4.32 grams of $CaCL_2$ per 18 liters of water.
4. 165.5 grams of NaCL per 18 liters of water.

For all the tests conducted the specimens were immersed in a constant-temperature saline bath (Fig. 3.5). The temperature of the saline solution in the one-cubic-inch plexiglas bath was controlled by circulating water from a six gallon constant temperature source through a small copper heat-exchanger coil placed in the saline solution. The source temperature was automatically controlled at a specified temperature by a Bronwill Model 20 Constant-Temperature Circulator. A calibration of this system at room temperature indicated that the temperature of the saline bath could be held at 37 ± 1° C. by circulating water at 40° C. through the heat exchanger. A complete calibration of the system between source temperatures of 23° C. and 50° C. indicated a linear relationship with the temperature of the saline bath. The temperature of the saline bath was measured with a thermocouple. In order to get a sufficient sensitivity at these low temperatures, the transducer was composed of three

copper-constantan thermocouples wired in series. The reference junction for this thermocouple was held constant by immersion in a saline solution at room temperature. The bath temperature was then measured as a difference from the room temperature on a Bristol millivolt strip chart recorder (Fig. 3.6).

The grips used to secure the specimens in the testing fixtures were similar to the snubbing type used for the testing of metal wire samples (Fig. 3.7). In these devices the specimens were clamped and then wrapped around one-quarter of the cylinder. The gauge length of 3 centimeters used for these tests was measured from the tangent points on the upper and lower grips. This gauge length was measured with a travelling microscope which had two Scherr Tumico dial gauges, graduated in 0.001 inch intervals, attached to it (Fig. 3.6). This device was also used to measure the diameters of the samples. The diameters were measured by moving the microscope lens horizontally with a micrometer graduated in 0.002 millimeter intervals. Because of variations of as much as twenty percent in the diameter of some specimens down the length, readings were taken at ten different points. By assuming the specimens to have a circular cross-section, the area of the sample was determined by averaging the areas obtained at the ten different locations.

Two different testing fixtures were used for these tests. The first fixture was used for tests which required a constant rate of strain (Fig. 3.8). Except for its size, it is similar to other tensile testing machines. The crosshead is driven at a constant rate by the turning of two fine threaded screws which are mounted in stainless steel ball bearings. Inserted into the stationary upper plate is a Statham Model UC3 Universal Transducing Cell adapted with a Statham UL4-0.5 load cell accessory. This cell was powered by a Statham Model SC1001 Universal Transducer Readout unit. Displacements of the crosshead were measured with a stainless steel clip gauge inserted between the crosshead and the load cell plate. The clip gauge was constructed from a strip of stainless steel 0.008 inches thick and 0.20 inches wide with two SR-4 strain gauges attached to either side. The strain gauges, Micro-Measurements Model EA-06-062AQ-350, were coated with Gagekote #5. This clip gauge was used with an Ellis Associates Model BAM-1 Bridge Amplifier Meter. A second fixture was used for the sinusoidal tests. This fixture is basically a variable amplitude scotch yoke, which is capable of inducing sinusoidal displacements with amplitudes from zero to one inch (Fig. 3.9).

Three basic test patterns were performed on the collagen bundles. Before each test the specimen was cycled once to align and tighten the sample in the grips.

This was accomplished by adjusting the initial length of the specimen until it just began to pick up a load. The first series of tests were relaxation experiments. The specimens were loaded at a certain rate of strain to a predetermined level of strain and held for a certain period of time.

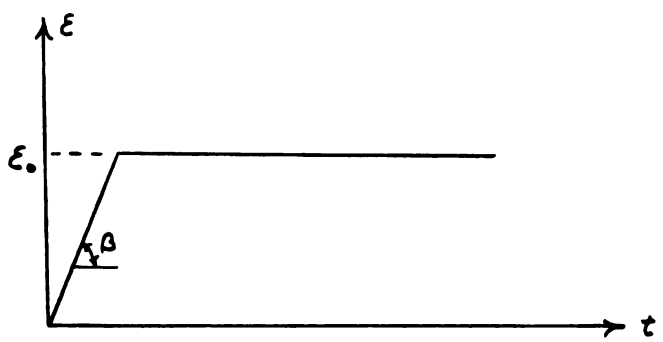

Fig. 3.1 Experimental Stress Relaxation Test

The load and displacement of the specimen was monitored on a Sanborn Model 60-1300 Twin Viso strip chart recorder equipped with two Sanborn Model 64-300A d.c. amplifiers. The second series of tests consisted of a number of loading and unloading cycles at different strain rates.

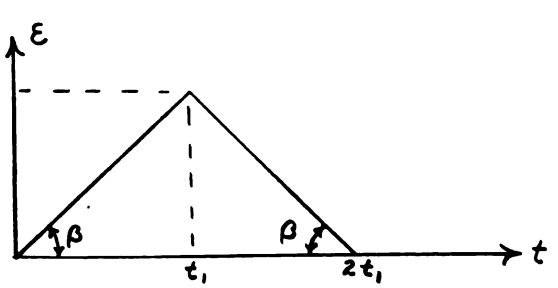

Fig. 3.2 Cyclic Test

For these tests a Varian F-80 x-y Recorder plotted the load-displacement curve for each cycle. The third series of tests involved the use of the scotch yoke to induce sinusoidal displacements in the specimen. For each experiment the yoke was started at the low point in its cycle, so that all strains were positive.

Fig. 3.3 Sinusoidal Test

These experiments were performed for various frequencies and amplitudes of displacement. The Sanborn recorder was used to plot the load and displacement simultaneously with time.

Both testing fixtures were driven by a 1/70 horsepower Bodine Model NSR-12R shunt wound motor. The speed of the motor was controlled with a Minarik Model W-14 speed control unit. In order to obtain low rates of displacement without reducing the motor speed significantly, the test apparatus included a gearbox designed for 5 to 1, 3 to 1, and 1 to 1 speed reductions.

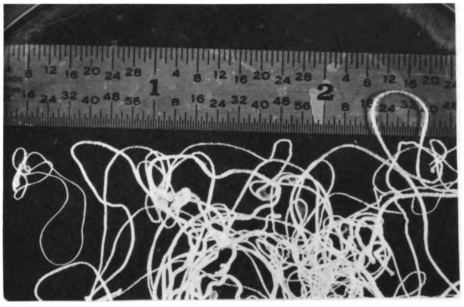

Fig. 3.4--Collagen Fiber Bundles

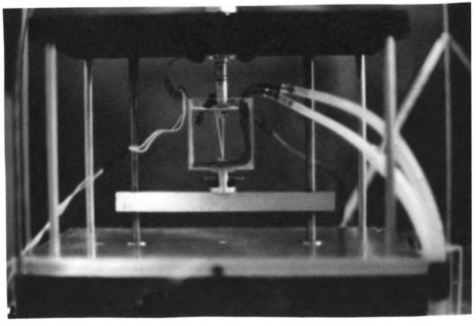

Fig. 3.5--Fiber Immersed in Saline Bath

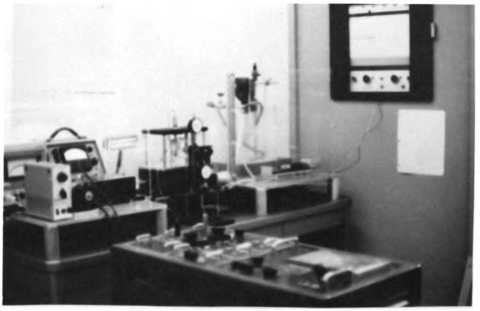

Fig. 3.6--Experimental Setup

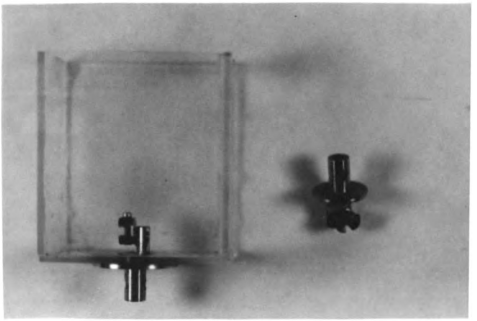

Fig. 3.7--Specimen Drips

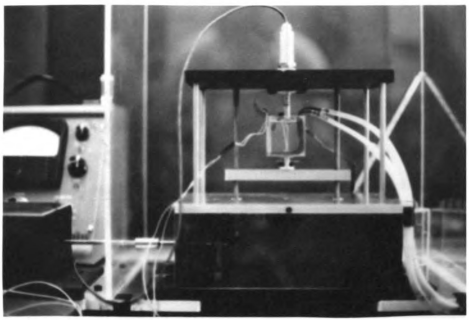

Fig. 3.8--Tensile Testing Fixture

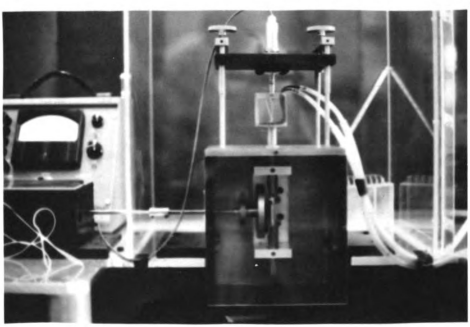

Fig. 3.9--Sinusoidal Test Fixture

IV. MATHEMATICAL FORMULATION

It has been suggested in the literature that time effects must be included in the formulation of a constitutive equation for biological tissues and various models have been proposed which involve the use of a discrete model analysis. However, these models have failed to adequately predict the results of experimentation. Rather than to attempt a mathematical formulation which involves the use of nonlinear springs and dashpots, the author feels a better result might be reached by using a stress-strain-history law in the form of a hereditary integral. This type of equation has been proposed by Y. C. Fung in the form

$$\sigma(t) = \int_0^t G(t-t') \frac{d\sigma^e[\lambda(t')]}{d\lambda} \frac{d\lambda(t')}{dt'} dt' \qquad 4.1$$

where σ^e is an "elastic" response, λ is the extension ratio, and G(t) is a "reduced" relaxation function. Since this study uses strains instead of extension ratios, the equation will be written as

$$\sigma(t) = \int_0^t G(t-t') \frac{d\sigma^e[\varepsilon(t')]}{d\varepsilon} \frac{d\varepsilon(t')}{dt'} dt' \qquad 4.2$$

where G(t) is a "reduced" relaxation function. Fung proposes that the "elastic" stress for rabbit mesentery may be written as

$$\sigma^e = D[\lambda - \frac{1}{\lambda^2}]e^{b\lambda} \qquad 4.3$$

where D and b are constants. If we describe the Lagrangian strain by

$$\varepsilon = \frac{L-L_o}{L_o} = \lambda - 1 \qquad 4.4$$

Fung's elastic equation may be written as

$$\sigma^e = K[\varepsilon - \varepsilon^2]e^{b\varepsilon} \qquad 4.5$$

For small strain this equation reduces to

$$\sigma^e = K[\varepsilon + (b-1)\varepsilon^2 + \ldots] \qquad 4.6$$

H. Elden describes this equation in his work on rat dermis, where the second term is due largely to the tension of collagen fibers. For a study of rat tail tendons it is then reasonable to assume that the "elastic" equation should be of the form

$$\sigma^e = C'\varepsilon^2 \qquad 4.7$$

for collagen fibers.

In some preliminary tests on the relaxation of biological tissues it has been seen that the stress relaxes as a linear function of the logarithm of time (9,26, 28). Assuming this to follow in Fung's hereditary integral,

the "reduced" relaxation function should also be linearly dependent on the logarithm of time.

$$G(t) = A' \ell n t + B' \tag{4.8}$$

Substitution of this information into the nonlinear hereditary integral yields,

$$\sigma(t) = E \int_0^t [\mu \ell n(t-t')+1]\varepsilon(t') \frac{d\varepsilon(t')}{dt'} dt' \tag{4.9}$$

where $E = 2B'C'$ and $\mu = \frac{A'}{B'}$.

1. Relaxation Test

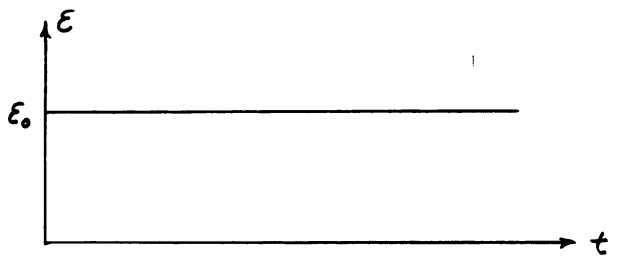

In a relaxation test the strain is given by $\varepsilon = \varepsilon_o H(t)$ where $H(t)$ is a unit step function. The derivative of this expression is

$$\frac{d\varepsilon}{dt} = \varepsilon_o \delta(t)$$

where $\delta(t)$ is the Dirac delta function. Substitution into the Equation 4.9 yields

$$\sigma(t) = E\varepsilon_o^2 \int_0^t [\mu \ell n(t-t')+1]\delta(t')dt' \tag{4.10}$$

The value of this integral is

$$\sigma(t) = E\varepsilon_o^2 [\mu \ell n t + 1] \qquad 4.11$$

for the stress response of a relaxation test.

2. Constant Strain Rate Test

For a constant strain rate test the strain can be written as $\varepsilon = \beta t$, where β is the strain rate (Fig. 3.2). Substitution of the strain expression into Equation 4.9 yields

$$\sigma(t) = E\beta^2 \int_0^t [\mu \ell n(t-t') + 1] t' dt' \qquad 4.12$$

or integrating

$$\sigma(t) = \frac{E\beta^2 t^2}{2} + \mu E\beta^2 \int_0^t t' \ell n(t-t') dt'$$

The second integral may be evaluated by letting $x = t-t'$ yielding

$$\sigma(t) = \frac{E\beta^2 t^2}{2} + \mu E\beta^2 \int_0^t (t-x) \ell n x dx$$

or after integrating

$$\sigma(t) = \frac{E\beta^2 t^2}{2} + \mu E\beta^2 [t^2 \ell n t - t^2 - \frac{t^2}{2} \ell n t + \frac{t^2}{4}]_0^t .$$

The lower limit of this expression behaves as

$$\lim_{t \to 0} t^2 \ell n t ,$$

which by L'Hospital's rule is equal to zero in the limit. Therefore, the stress response to a constant strain rate test using the hereditary integral Equation 4.9 is given by

$$\sigma(t) = \frac{E\beta^2 t^2}{2} + \mu E\beta^2 [\frac{t^2}{2} \ell n t - \frac{3}{4} t^2] \qquad 4.13$$

or rewriting in terms strain

$$\sigma(\varepsilon) = \frac{E\varepsilon^2}{2} + \frac{\mu E}{2} [\varepsilon^2 \ell n (\frac{\varepsilon}{\beta}) - \frac{3}{2}\varepsilon^2] \qquad 4.14$$

If one considers a test in which the strain increases linearly with time to a certain level and then is reversed, the strain can be written as

$$\varepsilon(t) = \begin{cases} \beta t \text{ for } 0 \leq t \leq t_1 \\ 2\beta t_1 - \beta t \text{ for } t_1 \leq t \leq 2t_1 \end{cases}$$

where t_1 is the time when the strain is reversed (Fig. 3.2). Substitution of this strain expression into Equation 4.9 gives

$$\sigma(t) = E\beta^2 \int_0^{t_1} [\mu \ell n (t-t')+1] t' dt' - E\beta^2 \int_{t_1}^{t} [\mu \ell n (t-t')+1] (2t_1 - t') dt'.$$

This equation may be written as

$$\sigma(t) = E\beta^2 \int_0^{t} [\mu \ell n (t-t')+1] t' dt' - 2E\beta^2 t_1 \int_{t_1}^{t} \mu \ell n (t-t')+1] dt'$$

The first integral is exactly the same as Equation 4.12. By letting x = t-t' in the second integral, the equation becomes

$$\sigma(t) = \frac{E\beta^2 t^2}{2} + \mu E\beta^2[\frac{t^2}{2}\ell n\, t-\frac{3}{4}t^2]-2E\beta^2 t_1(t-t_1)$$
$$-2E\beta^2 t_1\mu \int_0^{t-t_1} \ell n\, x dx.$$

Integrating this equation yields

$$\sigma(t) = \frac{E\beta^2 t^2}{2} + \mu E\beta^2[\frac{t^2}{2}\ell n\, t-\frac{3}{4}t^2]-2E\beta^2 t_1(t-t_1)$$
$$-2E\beta^2\mu t_1(t-t_1)[\ell n\,(t-t_1)-1]$$

or

$$\sigma(t) = \frac{E\beta^2 t^2}{2} + \mu E\beta^2[\frac{t^2}{2}\ell n\, t-\frac{3}{4}t^2]-2E\beta^2 t_1(t-t_1)$$
$$\{1+\mu[\ell n\,(t-t_1)-1]\} \text{ for } t > t_1. \qquad 4.15$$

3. Sinusoidal Test

For the sinusoidal test as shown in Fig. 3.3, the strain is given by

$$\varepsilon = \frac{\varepsilon_o}{2}(1-\cos\omega t)$$

for amplitude ε_o and frequency ω. Substitution into the hereditary integral yields

$$\sigma(t) = \frac{E\varepsilon_o^2\omega}{4} \int_0^t [\mu \ell n(t-t')+1]\sin\omega t'(1-\cos\omega t')dt'$$

This equation may be written as

$$\sigma(t) = \frac{E\varepsilon_o^2\omega}{4} \int_0^t [\mu \ell n(t-t')+1]\sin\omega t'dt' - \frac{E\varepsilon_o^2\omega}{8}$$

$$\int_0^t [\mu \ell n(t-t')+1]\sin 2\omega t'dt'$$

by using the trigonometric identity $\sin 2\omega t = 2\sin\omega t\cos\omega t$, integration then yields

$$\sigma(t) = \frac{E\varepsilon_o^2}{16}[\cos 2\omega t-1] - \frac{E\varepsilon_o^2}{4}[\cos\omega t-1] +$$

$$\frac{E\varepsilon_o^2\omega}{4} \int_0^t \mu \sin\omega t' \ell n(t-t')dt' - \frac{E\varepsilon_o^2\omega}{8} \int_0^t \mu \sin 2\omega t'$$

$$\ell n(t-t')dt'.$$

By changing the variables to $x = t-t'$ and using the trigonometric identity for the difference of two angles, this equation may be written as

$$\sigma(t) = \frac{E\varepsilon_o^2}{16}[\cos 2\omega t-1] - \frac{E\varepsilon_o^2}{4}[\cos\omega t-1] + \mu\frac{E\varepsilon_o^2\omega}{4}\sin\omega t$$

$$\int_0^t \cos\omega x \ell n x dx - \mu\frac{E\varepsilon_o^2}{4}\cos\omega t \int_0^t \sin\omega x \ell n x dx$$

$$- \mu\frac{E\varepsilon_o^2\omega}{8}\sin 2\omega t \int_0^t \cos 2\omega x \ell n x dx + \mu\frac{E\varepsilon_o^2\omega}{8}\cos 2\omega t$$

$$\int_0^t \sin 2\omega x \ell n x dx. \qquad 4.16$$

If one examines the first integral, integration by parts yields

$$\int_0^t \cos\omega x \ln x\,dx = \frac{1}{\omega}\,[\ln x \sin\omega x]_0^t - \frac{1}{\omega}\int_0^t \frac{\sin\omega x}{x}dx$$

$$= \frac{1}{\omega}\ln t \sin\omega t - \frac{1}{\omega}[\frac{\pi}{2} + si(\omega t)], \qquad 4.17$$

where $si(\omega t)$ is the sine integral. A similar examination of the second integral yields

$$\int_0^t \sin\omega x \ln x\,dx = -\frac{1}{\omega}\,[\ln x \cos\omega x]_0^t + \frac{1}{\omega}\int_0^t \frac{\cos\omega x}{x}dx. \qquad 4.18$$

This integral may be evaluated by using the definition of the cosine integral from Abramowitz and Stegun (30).

$$ci(x) = \gamma(\text{Euler's constant}) + \ln x + \int_0^x \frac{\cos z - 1}{z}dz$$

$$= \gamma + \lim_{x\to 0}\ln x + \int_0^x \frac{\cos z}{z}dz \qquad 4.19$$

The integral in 4.18 can be rewritten as

$$\int_0^t \frac{\cos\omega x}{x}dx = \int_0^{\omega t}\frac{\cos y}{y}dy$$

for $y = \omega x$.

Therefore, by using the above definition of the cosine integral Equation 4.18 reduces to

$$\int_0^t \sin\omega x \ln x\,dx = -\frac{1}{\omega}\ln t \cos\omega t + \frac{1}{\omega}\,[ci(\omega t) - \gamma]$$

$$+ \frac{1}{\omega}\lim_{x\to 0}[\ln x(\cos x - 1)].$$

Using L'Hospital's rule the limit term goes to zero, so that the integral becomes

$$\int_0^t \sin\omega x \ell n x dx = \frac{1}{\omega} [ci(\omega t) - \gamma - \ell n t \cos\omega t]. \qquad 4.20$$

In a similar manner, one obtains

$$\int_0^t \cos 2\omega x \ell n x dx = \frac{1}{2\omega} \ell n t \sin 2\omega t - \frac{1}{2\omega} [\frac{\pi}{2} + si(\omega t)] \qquad 4.21$$

and

$$\int_0^t \sin 2\omega x \ell n x dx = \frac{1}{2\omega} [ci(2\omega t) - \gamma - \ell n t \cos 2\omega t]. \qquad 4.22$$

Substitution of Equations 4.17,20,21,22 into Equation 4.16 yields,

$$\begin{aligned}
\sigma(t) = {} & \frac{E\varepsilon_o^2}{16} [\cos 2\omega t - 1] - \frac{\varepsilon_o^2 E}{4} [\cos\omega t - 1] \\
& + \frac{E\varepsilon_o^2}{4} \mu \sin\omega t \{\ell n t \sin\omega t + \frac{\pi}{2} + si(\omega t)\} \\
& + \frac{E\varepsilon_o^2}{16} \mu \cos 2\omega t \{-\ell n t \cos 2\omega t - \gamma + ci(\omega t)\} \\
& - \frac{E\varepsilon_o^2}{4} \mu \cos\omega t \{-\ell n t \cos\omega t - \gamma + ci(\omega t)\} \\
& - \frac{E\varepsilon_o^2}{16} \mu \sin 2\omega t \{\ell n t \sin 2\omega t + \frac{\pi}{2} + si(\omega t)\}, \qquad 4.23
\end{aligned}$$

for the equation of the stress response to a sinusoidal strain.

V. PRESENTATION OF RESULTS

The experimental results of the tests conducted on the collagen fibers are tabulated in Tables 1, 2, and 3. The general shape of the stress-strain equations was determined by observing that for a number of tests at various strain rates the stress could be represented by a power of the strain. In Table 2 the value of this power varied between approximately 1.8 and 2.1. Since this result held for all strain rates, a value of 2.0 for an "elastic" stress-strain equation appeared to be quite justified for collagen fibers.

The results of a number of relaxation tests for various levels of strain and different strain rates are given in Table 1. For all of the relaxation tests conducted on the fibers, it was found that the stress decayed as a linear function of the logarithm of time. Furthermore, the results indicated that values of the experimental constants did not vary with the magnitude of the strain rate used for ramp input. However, as in Equation 4.11 derived for the stress response of collagen to a relaxation test, the constants in these equations do depend on the level of strain. From Equation 4.11 the stress is given as

$$\sigma(t) = E\varepsilon_o^2 \mu \ell n t + E\varepsilon_o^2$$

where μ and E are material constants. Using the results tabulated in Table 1, the values of these material constants can be determined. By taking the average of the three tests at different strain rates for each level of strain, one finds that at

$$\varepsilon_o = 1.8\%$$

$$\mu = -.17$$

$$E = 13.6 \times 10^6 \text{ dynes/cm.}^2$$ (where $E\varepsilon_o^2$ at 7.6%/min. was not used)

at

$$\varepsilon_o = 1.2\%$$

$$\mu = -.24$$

$$E = 20.2 \times 10^6 \text{ dynes/cm.}^2$$

and at

$$\varepsilon_o = 0.6\%$$

$$\mu = -.28$$

$$E = 34.7 \times 10^6 \text{ dynes/cm.}^2$$

where μ is an "equivalent" time constant. Although there is a certain amount of variation among the three tests, the best approximation might be obtained by the average value. Thus, the values of the material constants E and μ will be given as

$$\mu = -0.23$$

$$E = 23 \times 10^6 \text{ dynes/cm.}^2$$

for collagen fibers.

It was observed for a number of tests at various strain rates, that a dependence of the stress-strain curves on the strain rate existed (Fig. 5.1). According to the proposed theory, this dependence should be of the form given by Equation 4.14

$$\sigma(\varepsilon) = \frac{E\varepsilon^2}{2} + \frac{\mu E\varepsilon^2}{2}\left[\ell n\left(\frac{\varepsilon}{\beta}\right) - \frac{3}{2}\right]$$

for the strain rate β. In Figures 5.2-7 a number of experimental tests have been compared with the theoretical prediction. In each of these figures the material constants derived from the relaxation data have been used in the plotting of the theoretical equation.

A further check on the validity of the hereditary integral is represented in Figures 5.8-10. These curves represent the results of three cyclic tests performed on rat tails at different strain rates. Each of these tests indicate that there is a considerable amount of hystersis involved in the response of collagen. The equation for the loading curve has been presented as

$$\sigma(t) = \frac{E\beta^2 t^2}{2} + \frac{\mu E\beta^2}{2}\left[t^2 \ell n\, t - \frac{3}{2}t^2\right]$$

for $t \leq t_1$, but for the unloading cycle the stress has been given in Equation 4.15 as

$$\sigma(t) = \frac{E\beta^2 t^2}{2} + \mu E\beta^2 \{\frac{t^2}{2} \ell n t - \frac{3}{4}t^2\} - 2E\beta^2 t_1(t-t_1)$$

$$\{1+\mu[\ell n(t-t_1)-1]\}$$

where βt_1 is the peak strain. Both of these equations have been plotted with the values of E and μ obtained from the relaxation test, and compared with the experimental curves.

A final test of the theory has been displayed in Figures 5.12-15. As indicated in Fig. 5.11, the stress amplitude decreases as the material is subjected to a sinusoidally varying strain. Since the tests were conducted such that the strain would always be positive, the strain input must be written as

$$\varepsilon = \frac{\varepsilon_o}{2}(1-\cos\omega t)$$

where ω is the frequency. In these tests the most consistent technique of reading the data was to determine the stress decay for times when the strain was a maximum. The data indicated that the peak stress decreased as a linear function of the logarithm of the cycle number, so that at all frequencies

$$\sigma_p = F - G\ell og_{10} n.$$

At the times when the strain was a maximum, it follows that

$$\cos\omega t = -1$$

$$\sin\omega t = 0$$

$$\sin 2\omega t = 0$$

$$\cos 2\omega t = 1 \quad \text{for } t = \frac{(2n-1)\pi}{\omega} \text{ where } n = 1,2,3,\ldots .$$

Substitution of these times into the theoretical result of Equation 4.23 yields

$$\sigma(t) = \frac{E\varepsilon_o^2}{2} + \frac{3}{16} E\varepsilon_o^2 \mu \ell n\, t' + \frac{5}{16} \mu E \varepsilon_o^2 [ci(\omega t) - \gamma]$$

where γ (Euler's constant) = 0.577. Again in this final comparison of theory and experiment, the material constants had values which were determined from the relaxation tests.

Table 1. Experimental Results of Relaxation Tests at Different Strain Levels

Strain	Strain Rate	$E\varepsilon_o^2\mu$	$E\varepsilon_o^2$
%	%/min.	$\frac{\text{dynes/cm.}^2}{\ell n \text{ min.}} \times 10^{-6}$	dynes/cm.^{2}x10^{-6}
1.8	41.0	-7.81	35.7
	7.6	-8.07	80.9
	4.8	-6.34	52.3
1.2	41.0	-6.81	21.2
	7.6	-6.81	30.6
	4.8	-7.64	35.6
0.6	41.0	-3.26	13.5
	7.6	-3.43	11.2
	4.8	-3.60	12.9

Table 2. Experimental Constants from Constant Strain Rate Tests ($\sigma = B\varepsilon^A$)

Strain Rate	A	B
%/min.		dynes/cm.^{2}x10^{-6}
1.1	2.07	18.7
3.6	1.81	20.8
8.1	1.81	22.2
9.2	2.06	19.9
10.9	2.00	18.0
12.8	1.82	20.4
18.7	1.80	22.2
22.6	1.78	26.4
26.7	1.85	25.5
30.9	1.87	23.3
34.8	1.93	23.3
37.5	2.00	22.4
45.0	1.83	28.3
50.9	1.90	31.4

Table 3. Experimental Constants from Sinusoidal Tests

Strain	Frequency	F	G
%	rad./min.	dynes/cm.^{2}x10^{-6}	dynes/cm.^{2}x10^{-6}
	3.3	65.8	43.9
	8.0	66.2	36.7
	15.1	75.1	42.3
	23.0	74.7	40.2
1.8	31.6	71.4	41.4
	52.1	93.2	46.3
	77.3	75.6	37.9
	101.0	91.3	43.0
	129.0	94.8	39.1
	77.3	75.2	31.9
	31.6	42.0	27.6
1.2	23.0	51.9	27.7
	15.1	41.0	23.5
	8.0	51.6	28.6
	77.3	23.9	10.2
	31.6	25.0	10.6
0.6	23.0	25.2	10.9
	15.1	25.2	12.8
	8.0	18.4	11.4

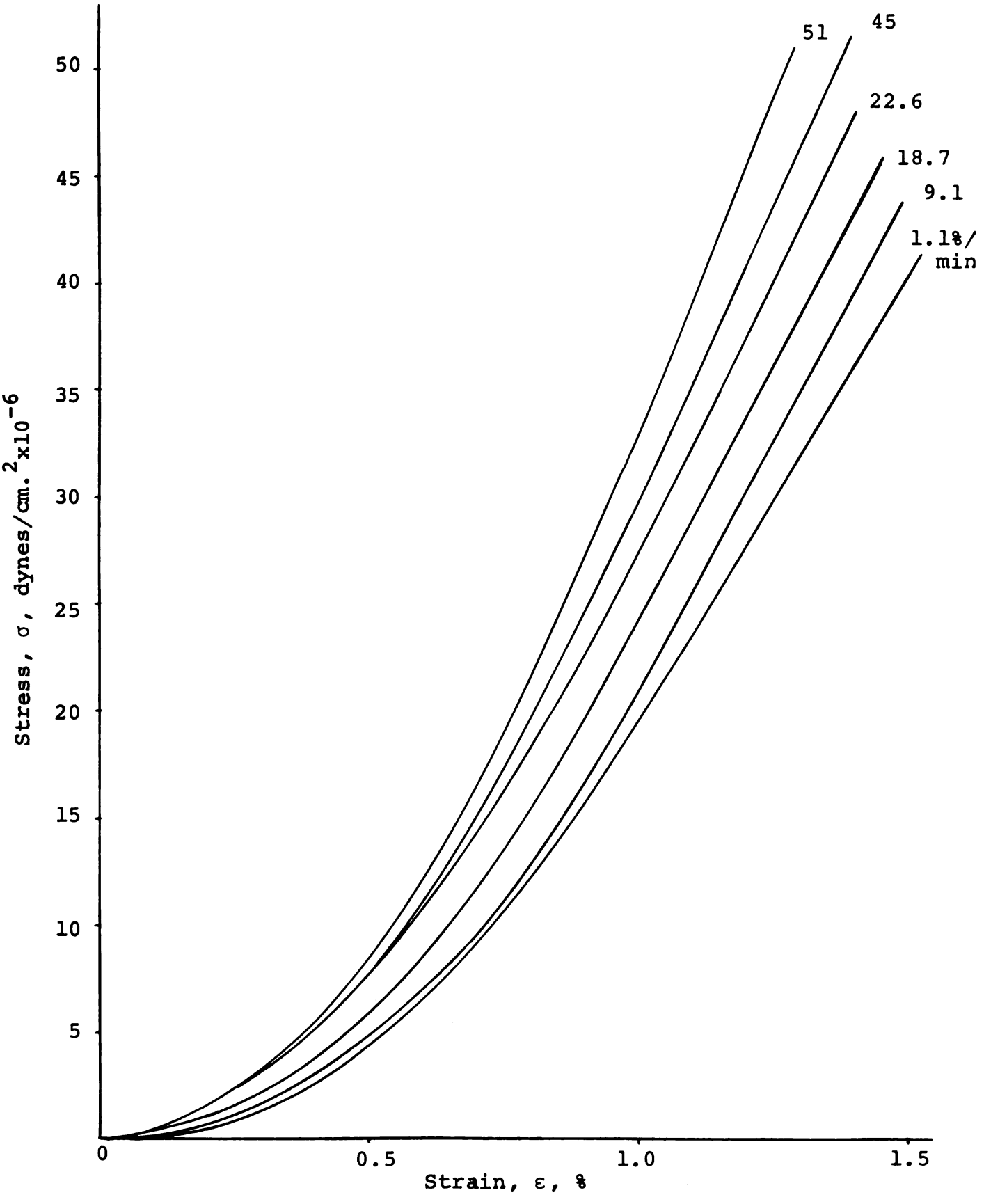

Fig. 5.1 Stress-Strain Plot at Various Strain Rates

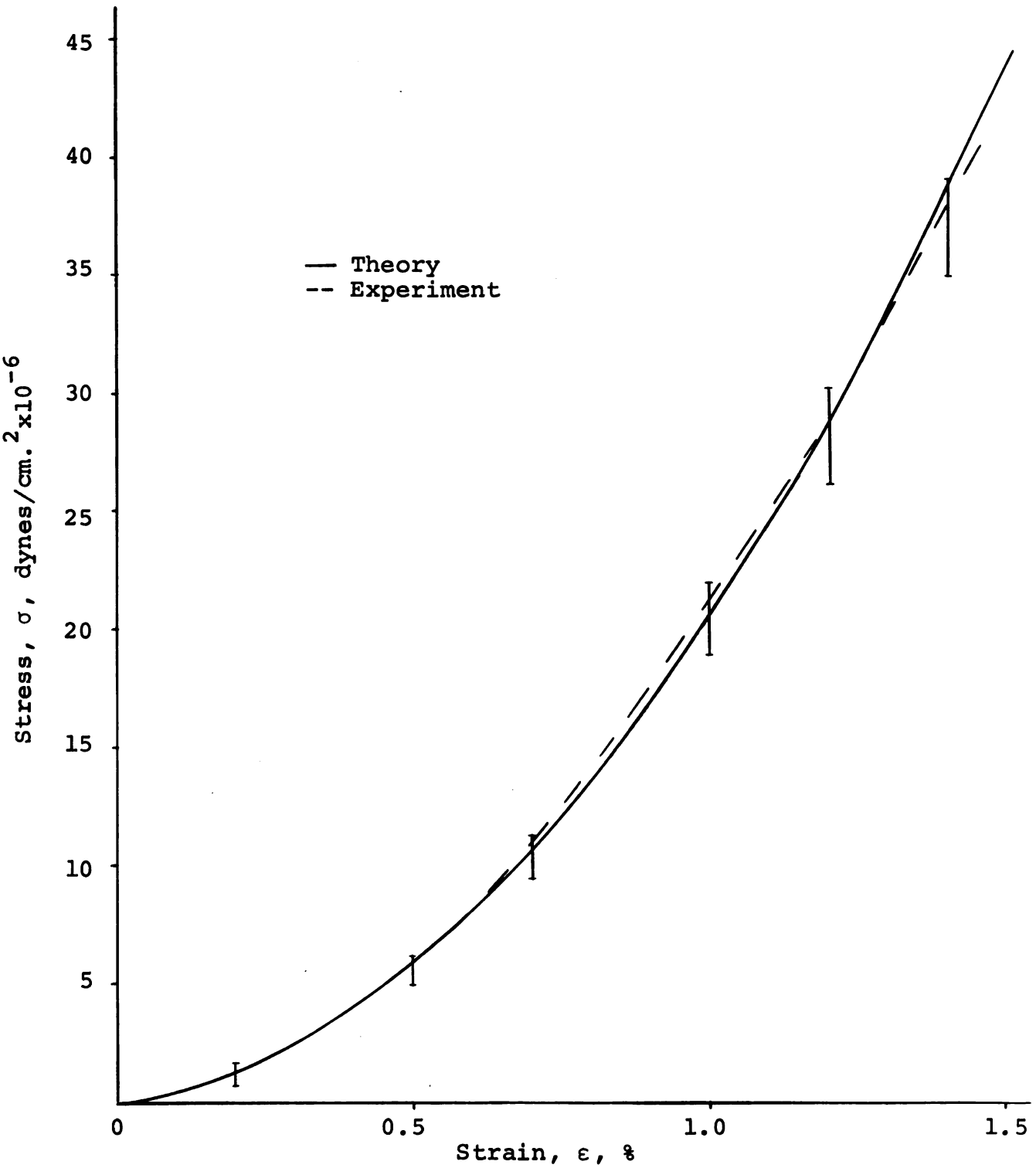

Fig. 5.2 Stress-Strain Plot for 3.6%/min. Strain Rate

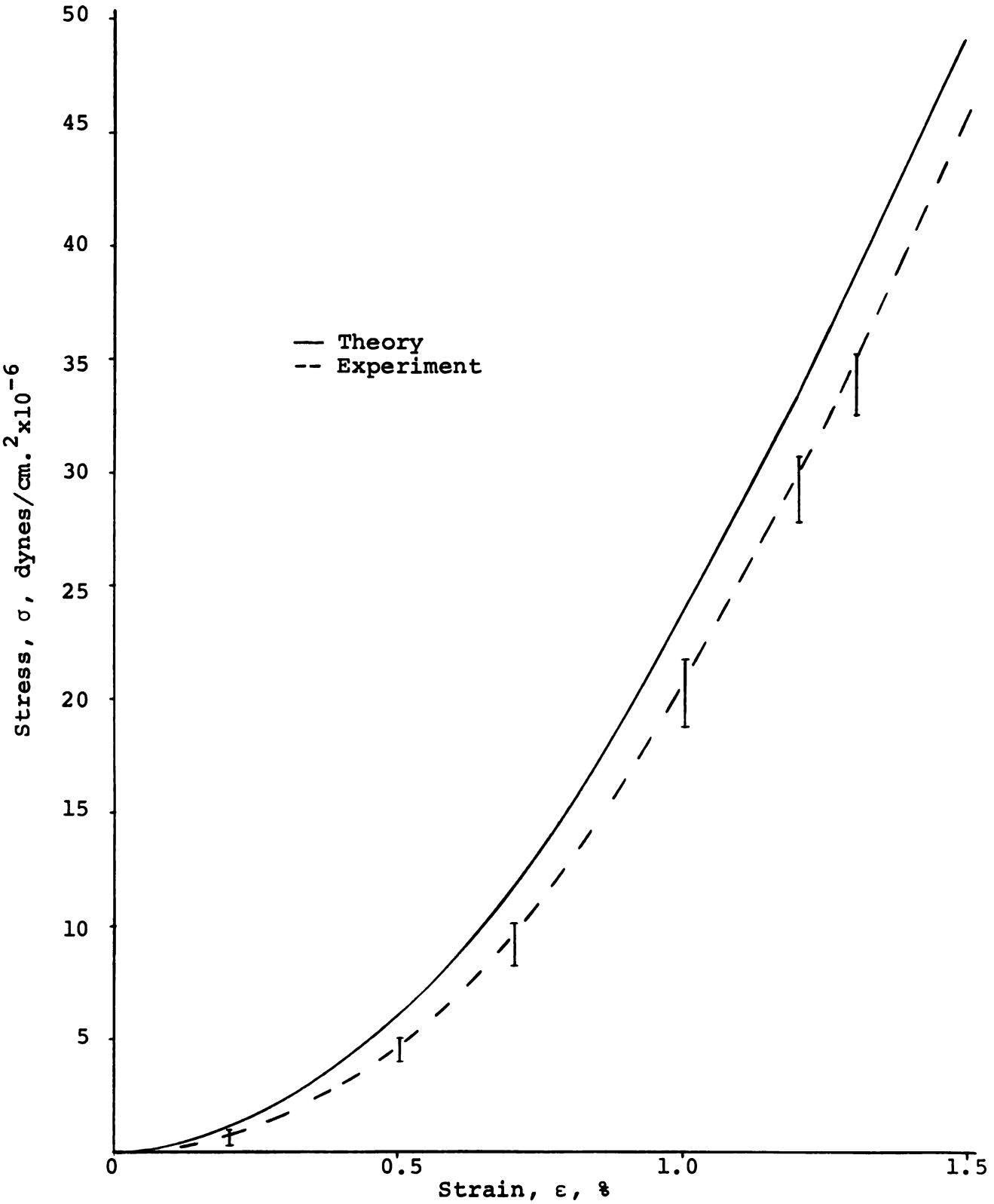

Fig. 5.3 Stress-Strain Plot for 9.2%/min. Strain Rate

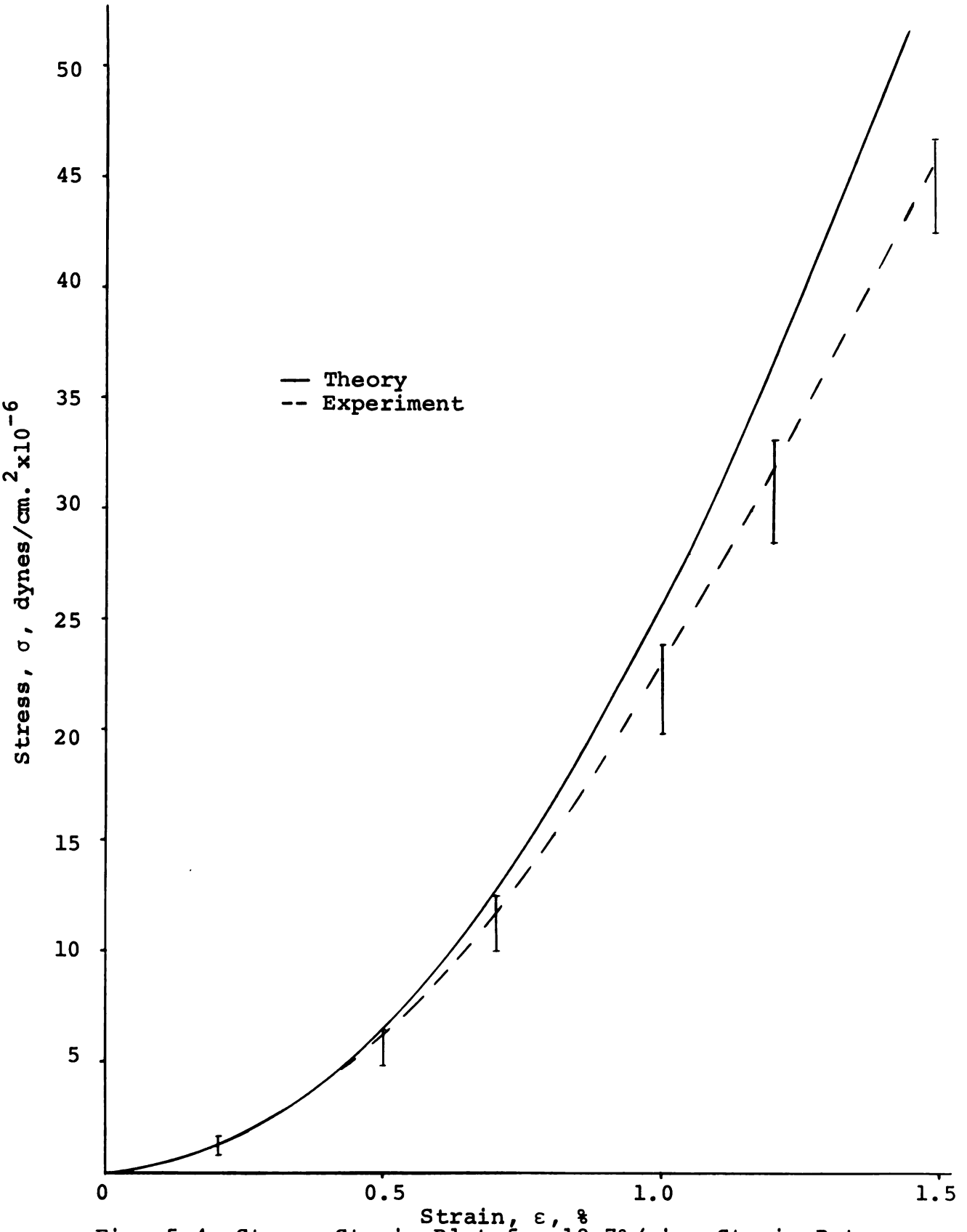

Fig. 5.4 Stress-Strain Plot for 18.7%/min. Strain Rate

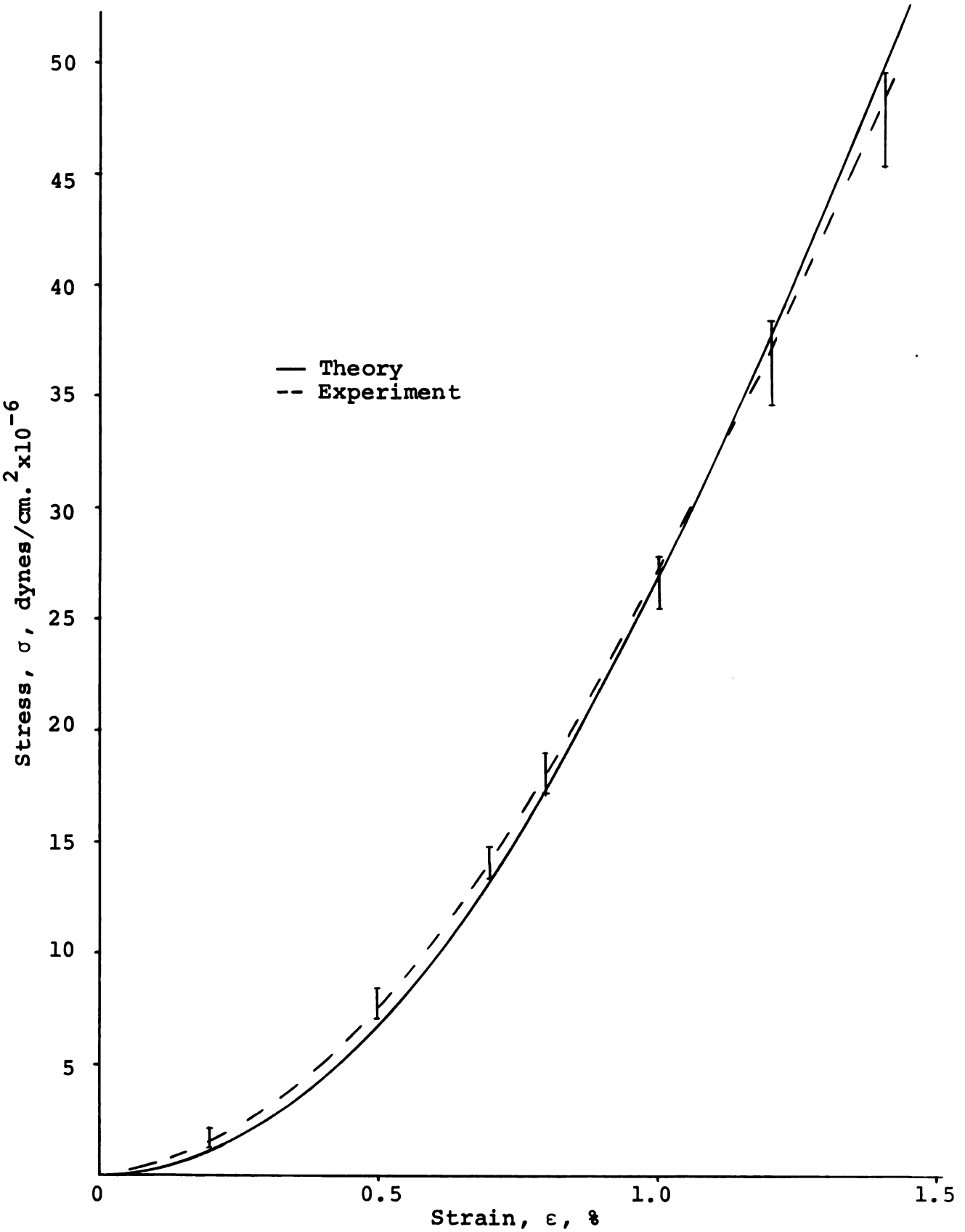

Fig. 5.5 Stress-Strain Plot for 22.6%/min. Strain Rate

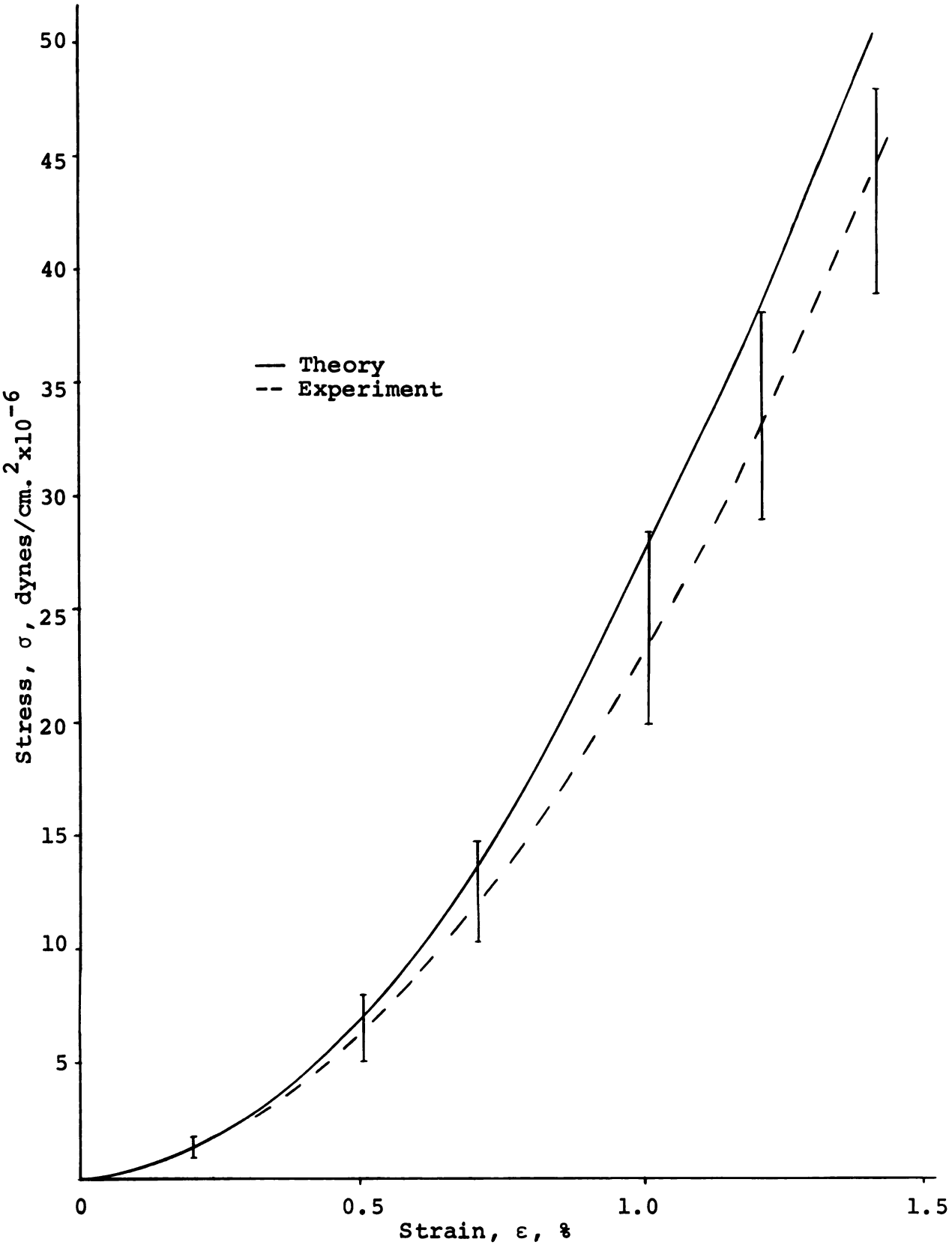

Fig. 5.6 Stress-Strain Plot for 30.9%/min. Strain Rate

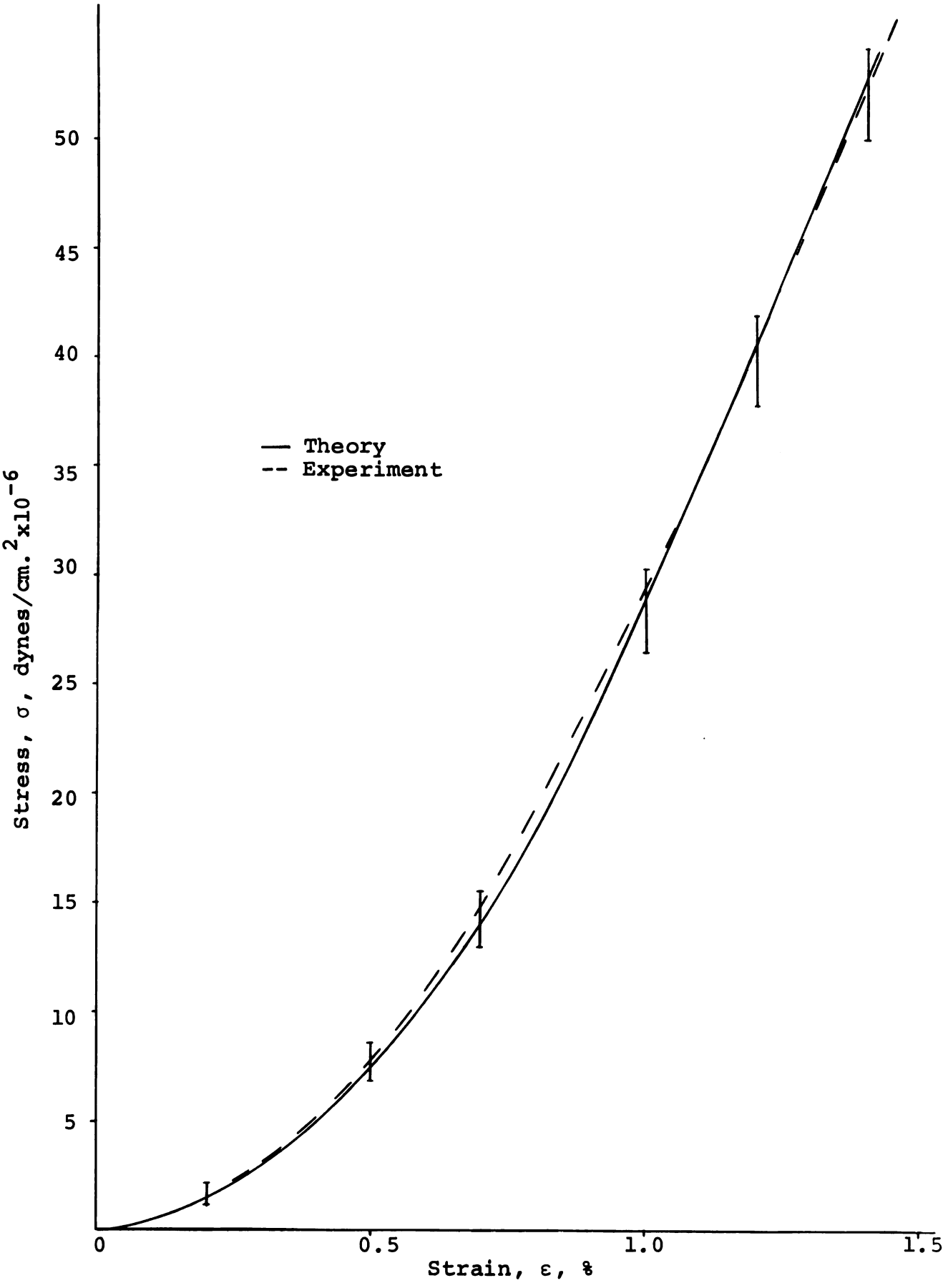

Fig. 5.7 Stress-Strain Plot for 45.0%/min. Strain Rate

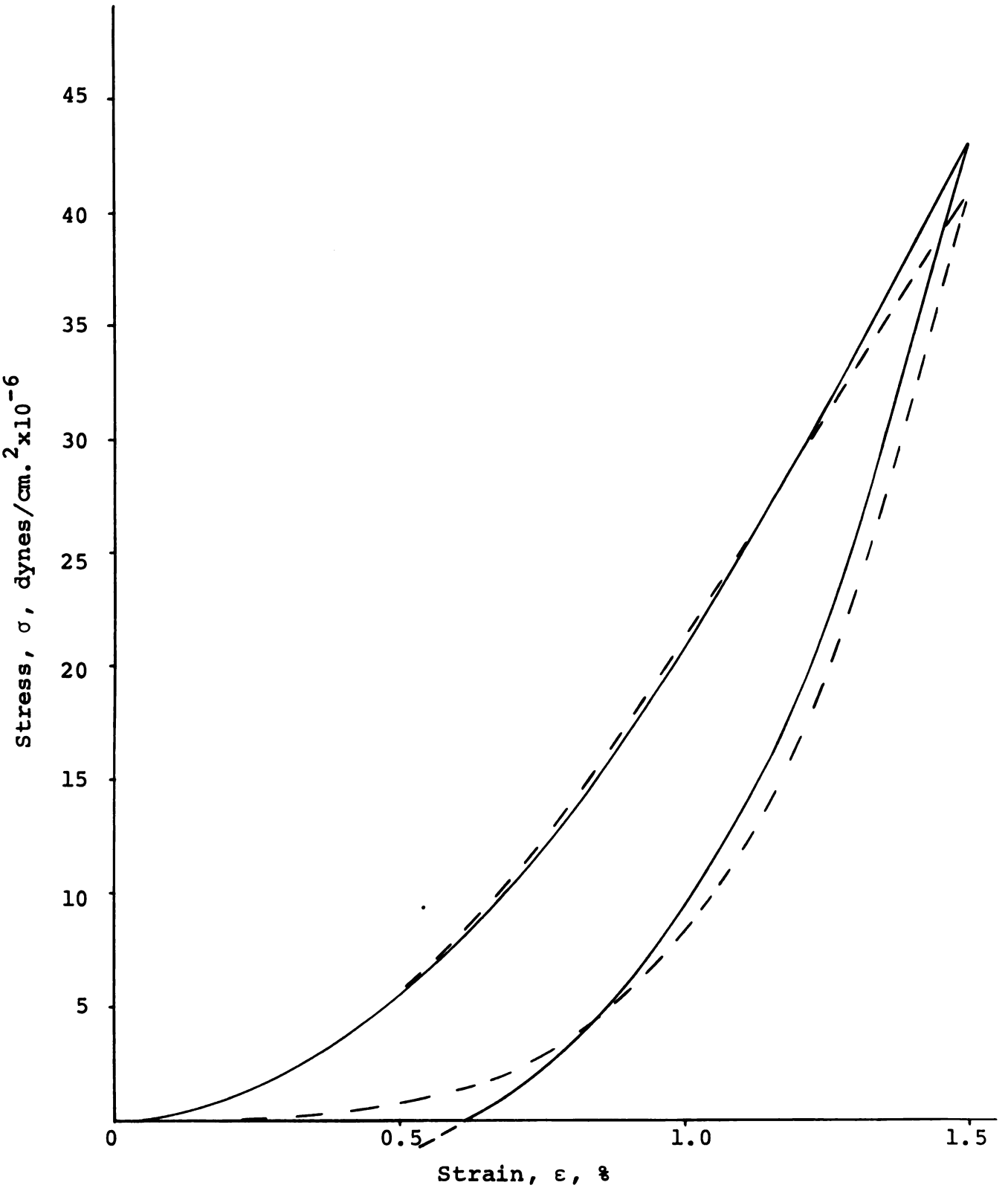

Fig. 5.8 Hysteresis Loop at 3.6%/min. Strain Rate

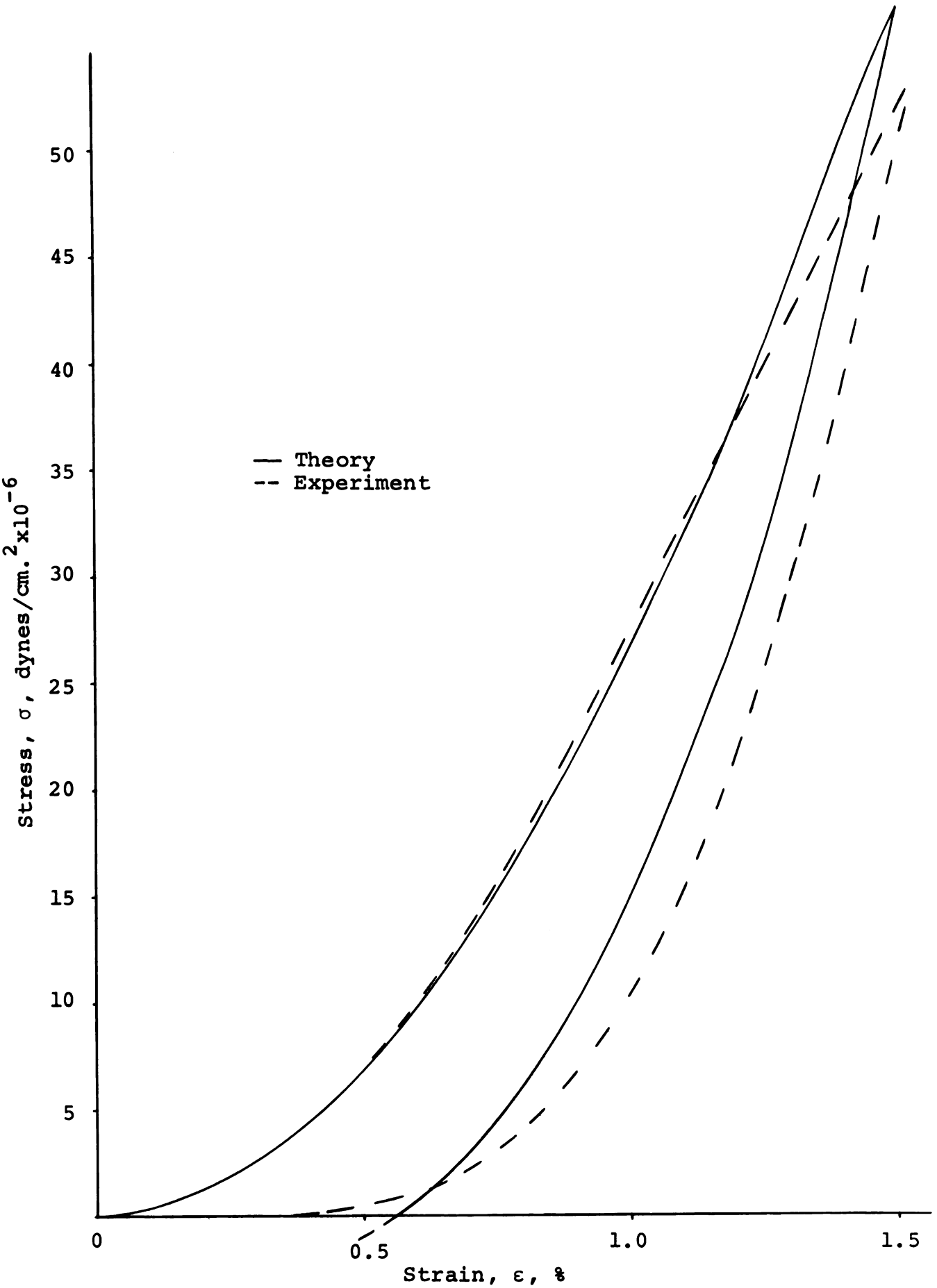

Fig. 5.9 Hysteresis Loop at 22.6%/min. Strain Rate

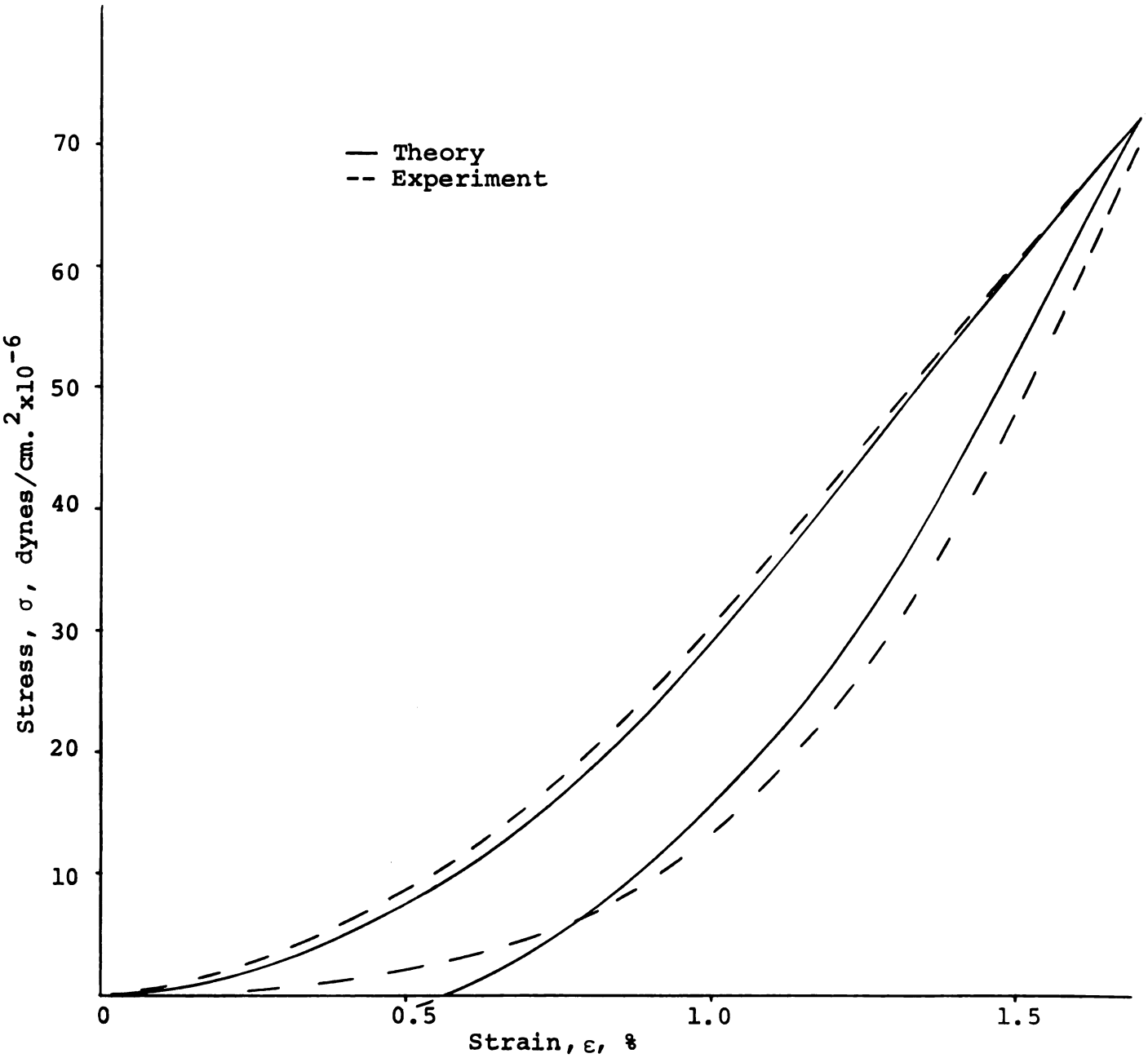

Fig. 5.10 Hysteresis Loop at 45.0%/min. Strain Rate

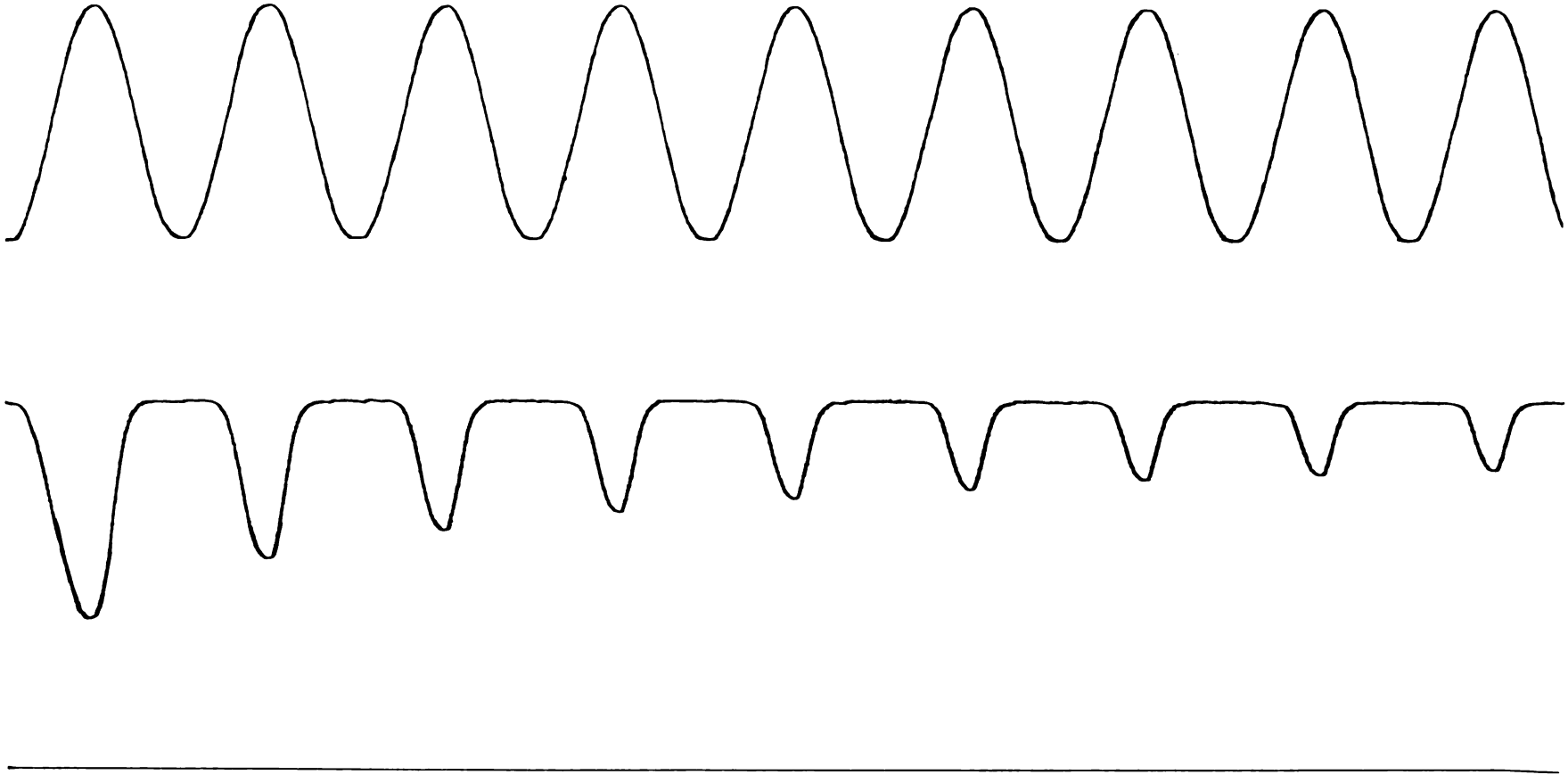

Fig. 5.11 Load Decay During Sinusoidal Extension

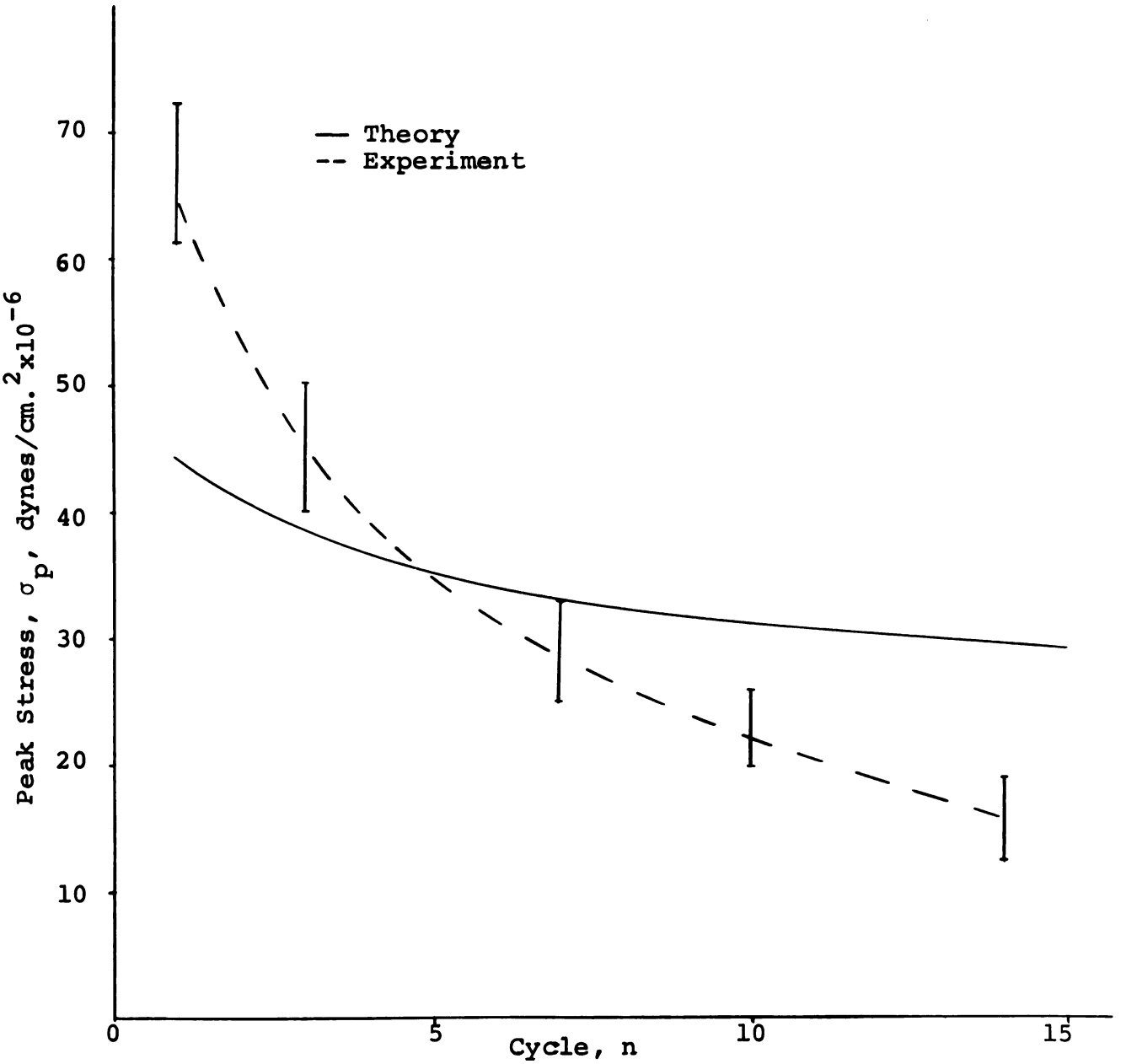

Fig. 5.12 Plot of Stress Amplitude vs. Cycle Number at a Frequency of 3.3 rad./min. and a Strain Amplitude of 1.8%

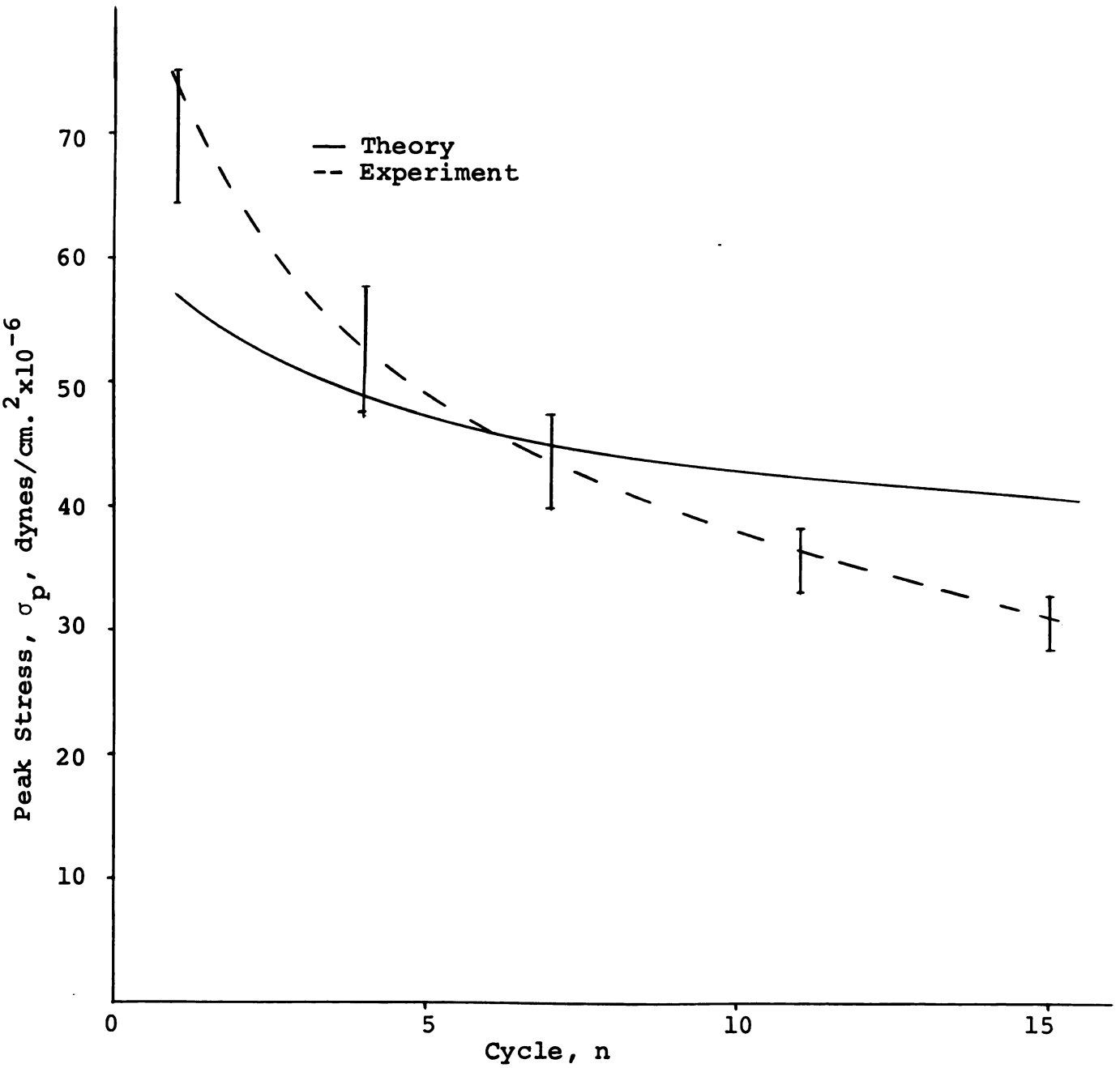

Fig. 5.13 Plot of Stress Amplitude vs. Cycle Number at a Frequency of 77.0 rad./min. and a Strain Amplitude of 1.8%

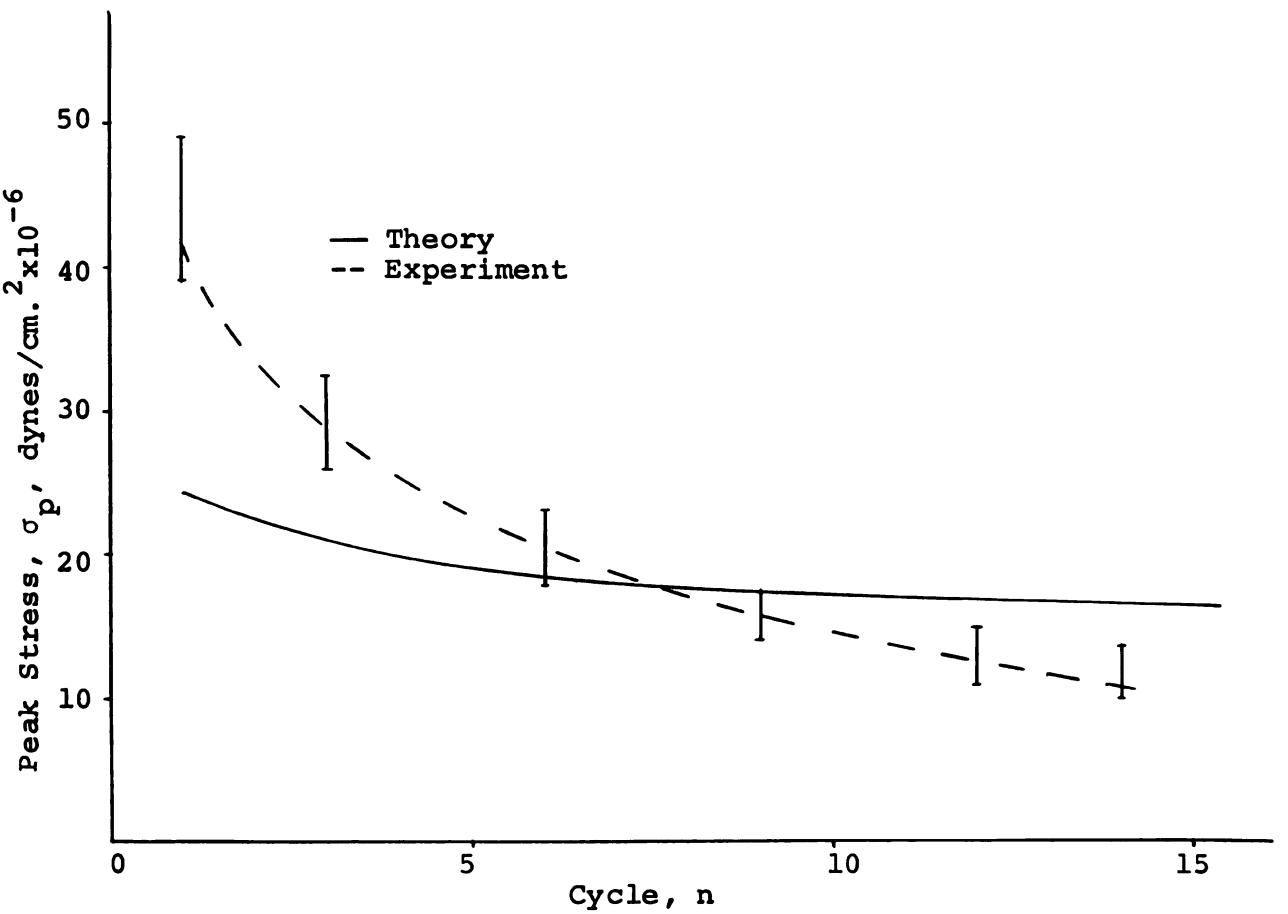

Fig. 5.14 Plot of Stress Amplitude vs. Cycle Number at a Frequency of 31.6 rad./min. and a Strain Amplitude of 1.2%

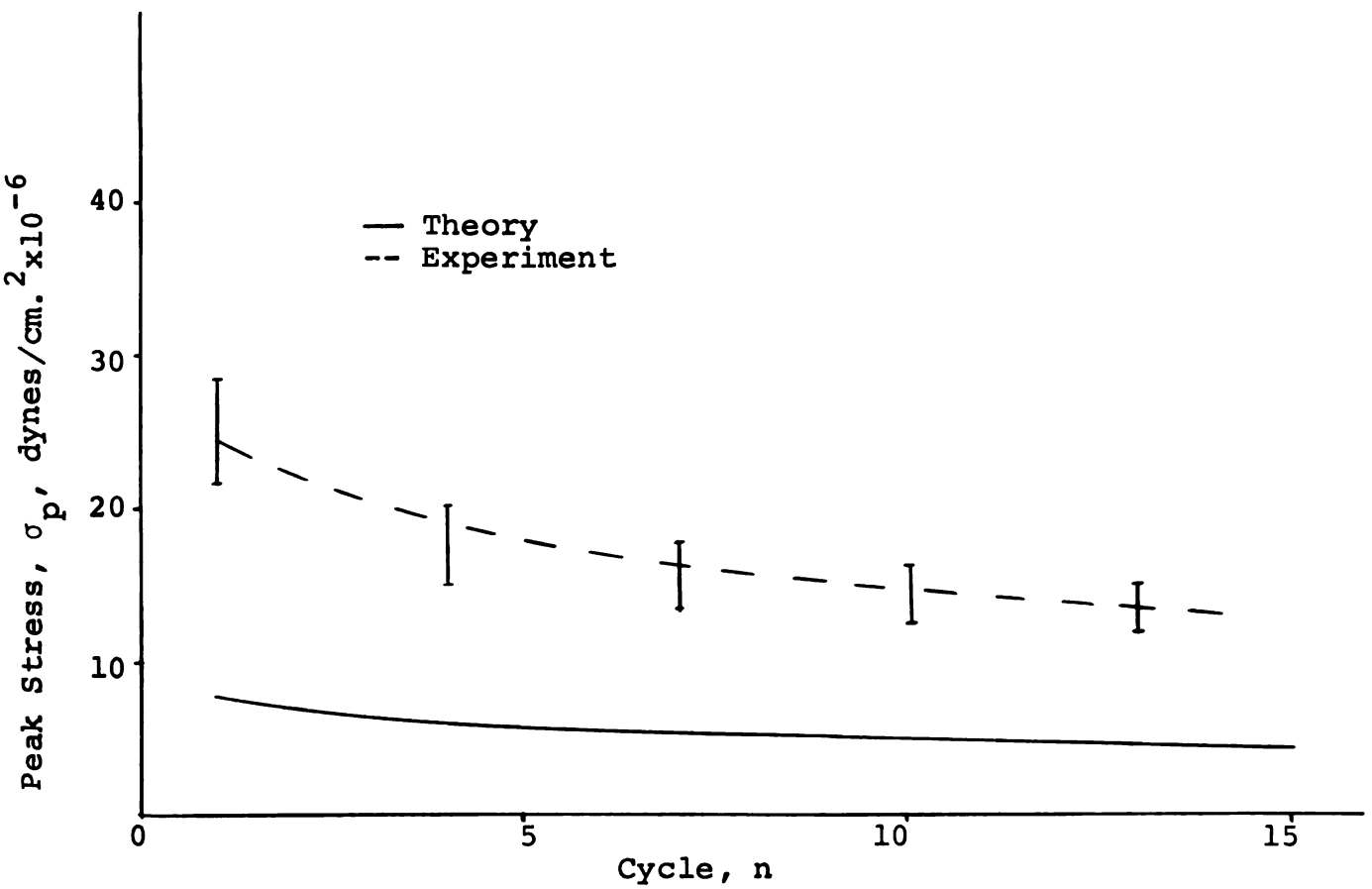

Fig. 5.15 Plot of Stress Amplitude vs. Cycle Number at a Frequency of 31.6 rad./min. and a Strain Amplitude of 0.6%

VI. CONCLUSIONS

A power function stress-strain law in the form of the square of the strain gave good agreement with these experiments on collagen fibers. This is in contrast to an exponential equation given by Fung for the mesentery. However, as stated earlier, the difference between these forms can be argued by a histological analysis of the tissues in question. As discussed previously, H. R. Elden has determined that the stress-strain response of skin can be given as the sum of a linear and squared term in strain, where the response of the collagen fibers is determined in the second nonlinear region. If one looks at the equation developed for the cyclic tests at constant strain rate, it becomes quite obvious that the term $\frac{E\varepsilon^2}{2}$ behaves as an elastic contribution to the entire cycle. Therefore, from the constants developed in the relaxation test, an apparent modulus of 11.5×10^6 dynes/cm.^{2} might be associated with this elastic term. In the literature Stromberg has given an apparent modulus of 8×10^6 dynes/cm.^{2} for rat tail tendons, and other authors have stated values of approximately 0.8×10^6 dynes/cm.^{2} for whole tendons.

The hereditary integral proposed in Equation 4.9 for collagen predicted the results of experiments at

constant strain rate very well. Although, the theoretical results did tend to be somewhat higher than experiment for a number of intermediate strain rates, the test results at both high and low strain rates were predicted very closely (Figures 5.2-7). In the cyclic tests for constant strain rates the theory predicts a return cycle somewhat higher than that which was obtained by experiment (Figures 5.8-10). However, it can be seen that this difference is probably the result of a higher value of stress at the peak strain than was observed in the experiments. The theory also predicts a region of compression for the cyclic test near 0.5% strain. Although no compression values were observed, the stress was nearly zero throughout this region.

The largest variation between experiment and theory was observed in the sinusoidal tests. Although the form of the equation is correct, the rate of decay of the logarithmic function is approximately three times too small. As a result of this factor, neither the initial peak stress nor the rate of decay compared favorably with experiment.

It is hoped that this research may serve as a basis for future studies on the mechanical properties of biological tissues. The response of collagen in other testing environments, such as a blood plasma, should be examined. Temperature was not considered to be a variable in this study, but according to the literature this parameter is very important for temperatures above 40° C. Future studies

should also incorporate a series of tests in which the specimens are subjected to various stress inputs. These tests could be in the form of creep and cyclic stress studies.

BIBLIOGRAPHY

BIBLIOGRAPHY

1. Gross, J., "Collagen," Sci. American, Vol. 204, No. 5, 1961, pp. 120-130.

2. Schmitt, F. O., J. Gross, and J. H. Highberger, "States of Aggregation of Collagen," Symp. Soc. Exptl. Biol., Vol. 9, 1955, pp. 148-162.

3. Elden, H. R., "Physical Properties of Collagen Fibers," International Review of Connective Tissue Research, Ed. by D. A. Hall, Vol. 4, 1968.

4. Viidik, A., "Biomechanics and Functional Adaptation of Tendons and Joint Ligaments," Studies on the Anatomy and Function of Bone and Joints, Ed. by F. G. Evans, Heidleberg, 1966, pp. 17-40.

5. Elliot, D. H., "Structure and Function of Mammalian Tendon," Biological Reviews, Vol. 40, 1965, pp. 392-421.

6. Ham, A. W., Histology, J. B. Lippincott Co., 5th Ed., 1965.

7. Hall, M. C., The Locomotor System--Functional Histology, C. C. Thomas, Springfield, Ill., 1965.

8. Verzar, F., "Aging of the Collagen Fiber," International Review of Connective Tissue Research, Vol. 2, 1964.

9. Rigby, B., N. Hirai, J. Spikes, and H. Eyring, "The Mechanical Properties of Rat Tail Tendon," J. of General Physiology, Vol. 43, 1959, pp. 265-283.

10. Cronkite, A. E., "The Tensile Strength of Human Tendons," Anat. Rec., Vol. 64, 1963, pp. 173-186.

11. Harris, E. H., L. B. Walker, and B. R. Bass, "Stress-Strain Studies in Cadaveric Tendon and an Anomaly in the Young's Modulus Thereof," Med. and Biol. Enging, Vol. 4, 1966, pp. 253-259.

12. Smith, J. W., "The Elastic Properties of the Anterior Cruciate Ligament of the Rabbit," J. of Anatomy, Vol. 88, 1954, pp. 369-380.

13. Viidik, A., and T. Lewin, "Changes in Tensile Strength Characteristics and Histology of Rabbit Ligaments Induced by Different Modes of Postmartal Storage," Acta. Orthop. Scandinav., Vol. 37, 1966, pp. 141-155.

14. Elden, H. R., and R. J. Boucek, "A Reaction of Water with Rat Tail Tendons (Hydration-Elongation)," Biochimica Et Biophysica Acta., Vol. 38, 1960, pp. 205-211.

15. Stucke, K., "Tendon Loads and Rupture in Animal Experiments," Chirug., Vol. 22, 1951, p. 16.

16. Harkness, R. D., "Collagen," Sci. Progr., London, Vol. 54, 1966, pp. 257-274.

17. La Ban, M. M., "Collagen Tissue: Implications of Its Response to Stress in vitro," Arch. Phys. Med. Rehabil., Vol. 43, 1962, pp. 461-466.

18. Morgan, F. R., "The Mechanical Properties of Collagen Fibers: Stress-Strain Curves," Soc. Leather Trades' Chemists, Vol. 44, 1960, pp. 170-181.

19. Blatz, P. J., "On the Mechanical Behavior of Elastic Animal Tissue," Trans. Soc. Rheology, Vol. 13, 1969, pp. 83-102.

20. Fung, Y. C. B., "Elasticity of Soft Tissues in Simple Elongation," Amer. J. of Physiology, Vol. 213, No. 6, 1967.

21. Stromberg, D. D., and C. A. Wiederhielm, "Viscoelastic Description of a Collagenous Tissue in Simple Elongation," J. of Applied Physiology, Vol. 26, No. 6, 1969.

22. Haut, R. C., and R. W. Little, "The Rheological Properties of Canine Anterior Cruciate Ligaments," J. of Biomechanics, Vol. 2, 1969, pp. 289-298.

23. Van Brocklin, J. D., and D. Ellis, "A Study of the Mechanical Behavior of Toe Extensor Tendons Under Applied Stress," Arch. of Physical Medicine and Rehabil., Vol. 46, 1965, pp. 369-373.

24. Viidik, A., "Experimental Evaluation of the Tensile Strength of Isolated Rabbit Tendons," Biomed. Eng., Vol. 2, 1967, pp. 31-36.

25. Frísen, M., M. Magi, L. Sonnerup, and A. Viidik, "Rheological Analysis of Soft Collagenous Tissue," J. of Biomechanics, Vol. 2, 1969, pp. 13-28.

26. Abrahams, M., "Mechanical Behavior of Tendon in vitro (A Preliminary Report)," Med. and Biol. Enging, Vol. 5, 1967, pp. 433-443.

27. Jaminson, C. E., R. D. Marangoni, and A. A. Glaser, "Viscoelastic Properties of Soft Tissue by Discrete Model Characterization," Trans. of ASME, Paper No. 67-WA/BHF-1.

28. Apter, J. T., "Correlation of Viscoelastic Properties with Microscopic Structure of Large Arteries," Circ. Res., Vol. 21, 1967, pp. 901-918.

29. Fung, Y. C. B., "Biomechanics (Its Scope, History and Some Problems of Continuum Mechanics in Physiology)," Appl. Mech. Rev., Vol. 21, No. 1, 1968.

30. Abramowitz, M., and I. A. Stregun, Handbook of Mathematical Functions, Nat. Bureau of Standards, 1964.